organs. Marrow cells are routinely aspirated from patients and are therefore one of the most clinically practical sources of stem cells in adults. BMS cells are easy to culture and grow so rapidly. Therefore, these autologous cells have few practical, ethical, or immunological barriers to their clinical application and are a promising basis for future novel therapies.

Acknowledgements We are grateful to Dr. Yoshiko Takahashi for xNoggin/MC BOS. We also thank A. Thomson for critically reviewing the manuscript, K. Sakurada, F. Konishi, S. Higashi, Y. Uchida, T. Takizawa, W. Ochiai, M. Yanagisawa, Y. Takahashi, Y. Izawa, M. Fukuma, J. Ozawa, M. Takamatsu, S. Kusakari, Y. Yamada and T. Yamada for advice, and A. Kaneko for technical advice and discussion. This work was supported by a grant from the Ministry of Education, Science and Culture, and by Keio University Special Grant-in-Aid for Innovative Collaborative Research Project.

References

Ashton, B.A., Allen, T.D., Howlett, C.R., Eaglesom, C.C., Hattori, A. and Owen, M. (1980) Formation of bone and cartilage by marrow stromal cells in diffusion chambers in vivo. Clin Orthop 151:294–307.

Bessey, O.A., Lowry, O.H. and Breck, M.J. (1946) A method for the rapid determination of alkaline phosphatase with cubic millimeters of serum. J Cell Biol 164:321–326.

Bjornson, C.R., Rietze, R.L., Reynolds, B.A., Magli, M.C. and Vescovi, A.L. (1999) Turning brain into blood: a hematopoietic fate adopted by adult neural stem cells in vivo. Science 283:534–537.

Brazelton, T.R., Rossi, F.M., Keshet, G.I. and Blau, H.M. (2000) From marrow to brain: expression of neuronal phenotypes in adult mice. Science 290:1775–1779.

Clarke, D.L., Johansson, C.B., Wilbertz, J., Veress, B., Nilsson, E., Karlstrom, H., Lendahl, U. and Frisen, J. (2000) Generalized potential of adult neural stem cells. Science 288:1660–1663.

Dexter, T.M., Allen, T.D. and Lajtha, L.G. (1977) Conditions controlling the proliferation of haemopoietic stem cells in vitro. J Cell Physiol 91:335–344.

Ferrari, G., Cusella-De Angelis, G., Coletta, M., Paolucci, E., Stornaiuolo, A., Cossu, G. and Mavilio, F. (1998) Muscle regeneration by bone marrow-derived myogenic progenitors. Science 279:1528–1530.

Fuchs, E. and Segre, J.A. (2000) Stem cells: a new lease on life. Cell 100:143–155.

Harigaya, K., Cronkite, E.P., Miller, M.E. and Shadduck, R.K. (1981) Murine bone marrow cell line producing colony-stimulating factor. Proc Natl Acad Sci USA 78:6963–6966.

Holliday, R. (1996) DNA methylation in eukaryotes: 20 years on. In: In: Russo, V.E.A., Martienssen, R.A., Riggs, A.D. (eds) Epigenetic mechanisms of gene regulation Cold Spring, Harbor Laboratory Press, pp 5–27.

Hughes, F.J., Collyer, J., Stanfield, M. and Goodman, S.A. (1995) The effects of bone morphogenetic protein-2 -4 and -6 on differentiation of rat osteoblast cells in vitro. Endocrinology 136:2671–2677.

Kawasaki, H., Mizuseki, K., Nishikawa, S., Kaneko, S., Kuwana, Y., Nakanishi, S., Nishikawa, S.I. and Sasai, Y. (2000) Induction of midbrain dopaminergic neurons from ES cells by stromal cell-derived inducing activity. Neuron 28:31–40.

Lamb, T.M., Knecht, A.K., Smith, W.C., Stachel, S.E., Economides, A.N., Stahl, N., Yancopolous, G.D. and Harland, R.M. (1993) Neural induction by the secreted polypeptide noggin. Science 262:713–718.

Leboy, P.S., Beresford, J.N., Devlin, C. and Owen, M.E. (1991) Dexamethasone induction of osteoblast mRNAs in rat marrow stromal cell cultures. J Cell Physiol 146:370–378.

Lim, D.A., Tramontin, A.D., Trevejo, J.M., Herrera, D.G., Garcia-Verdugo, J.M. and Alvarez-Buylla, A. (2000) Noggin Antagonizes BMP Signaling to Create a Niche for Adult Neurogenesis. Neuron 28:713–726.

Makino, S., Fukuda, K., Miyoshi, S., Konishi, F., Kodama, H., Pan, J., Sano, M., Takahashi, T., Hori, S., Abe, H., Hata, J., Umezawa, A. and Ogawa, S. (1999) Cardiomyocytes can be generated from marrow stromal cells in vitro. J Clin Invest 103:697–705.

Marusich, M.F., Furneaux, H.M., Henion, P.D., Weston, J.A. (1994) Hu neuronal proteins are expressed in proliferating neurogenic cells. J Neurobiol 25: 143–155.

Metcalf, D. (1985) The granulocyte-macrophage colony stimulating factors. Cell 43:5–6.

Mezey, E., Chandross, K.J., Harta, G., Maki, R.A. and McKercher, S.R. (2000) Turning blood into brain: cells bearing neuronal antigens generated in vivo from bone marrow. Science 290:1779–1782.

Nakashima, K., Yanagisawa, M., Arakawa, H. and Taga, T. (1999) Astrocyte differentiation mediated by LIF in cooperation with BMP2. FEBS Lett 457:43–46.

Nakashima, K., Takizawa, T., Ochiai, W., Yanagisawa, M., Hisatsune, T., Nakafuku, M., Miyazono, K., Kishimoto, T., Kageyama, R. and Taga, T. (2001) BMP2-mediated alteration in the developmental pathway of fetal mouse brain cells from neurogenesis to astrocytogenesis Proc Natl Acad Sci USA 98:5868–5873.

Petersen, B.E., Bowen, W.C., Patrene, K.D., Mars, W.M., Sullivan, A.K., Murase, N., Boggs, S.S., Greenberger, J.S. and Goff, J.P. (1999) Bone marrow as a potential source of hepatic oval cells. Science 284:1168–1170.

Pincus, D.W., Keyoung, H.M., Harrison-Restelli, C., Goodman, R.R., Fraser, R.A., Edgar, M., Sakakibara, S., Okano, H., Nedergaard, M. and Goldman, S.A. (1998) Fibroblast growth factor-2/brain-derived neurotrophic factor-associated maturation of new neurons generated from adult human subependymal cells. Ann Neurol 43:576–585.

Pittenger, M.F., Mackay, A.M., Beck, S.C., Jaiswal, R.K., Douglas, R., Mosca, J.D., Moorman, M.A., Simonetti, D.W., Craig, S. and Marshak, D.R. (1999) Multilineage potential of adult human mesenchymal stem cells. Science 284:143–147.

Pittenger, M.F., Mosca, J.D., McIntosh, K.R. (2000) Human mesenchymal stem cells: progenitor cells for cartilage bone, fat and stroma. Curr Top Microbiol Immunol 251:3–11.

Ribera, A.B. (1999) Potassium currents in developing neurons. Ann NY Acad Sci 868:399–405.

Ribera, A.B., Spitzer, N.C. (1992) Developmental regulation of potassium channels and the impact on neuronal differentiation. Ion Channels 3:1–38.

Rickard, D.J., Sullivan, T.A., Shenker, B.J., Leboy, P.S. and Kazhdan, I. (1994) Induction of rapid osteoblast differentiation in rat bone marrow stromal cell cultures by dexamethasone and BMP-2. Dev Biol 161:218–228.

Roberts, R., Gallagher, J., Spooncer, E., Allen, T.D., Bloomfield, F. and Dexter, T.M. (1988) Heparan sulphate bound growth factors: a mechanism for stromal cell mediated haemopoiesis. Nature 332:376–378.

Roy, N.S., Wang, S., Jiang, L., Kang, J., Benraiss, A., Harrison-Restelli, C., Fraser, R.A., Couldwell, W.T., Kawaguchi, A., Okano, H., Nedergaard, M. and Goldman, S.A. (2000) In vitro neurogenesis by progenitor cells isolated from the adult human hippocampus. Nat Med 6:271–277.

Sawamoto, K., Yamamoto, A., Kawaguchi, A., Yamaguchi, M., Mori, K., Goldman, S.A. and Okano, H. (2001) Visualization and direct isolation of neuronal progenitor cells by dual-color flow cytometric detection of fluorescent proteins. J Neurosci Res 65:220–227.

Schinstine, M. and Iacovitti, L. (1997) 5-Azacytidine and BDNF enhance the maturation of neurons derived from EGF-generated neural stem cells. Exp Neurol 144:315–325.

Smith, W.C. and Harland, R.M. (1992) Expression cloning of noggin, a new dorsalizing factor localized to the Spemann organizer in *Xenopus* embryos. Cell 70:829–840.

Sugimoto, T., Umezawa, A. and Hata, J. (1997) Neurogenic potential of Ewing's sarcoma cells. Virchows Arch 430:41–46.

Tonegawa, A. and Takahashi, Y. (1998) Somitogenesis controlled by Noggin. Dev Biol 202:172–182.

Tropepe, V., Hitoshi, S., Sirard, C., Mak, T.W., Rossant, J. and van der Kooy, D. (2001) Direct neural fate specification from embryonic stem cells: a primitive mammalian neural stem cell stage acquired through a default mechanism. Neuron 30:65–78.

Umezawa, A., Harigaya, K., Abe, H. and Watanabe, Y. (1990) Gap-junctional communication of bone marrow stromal cells is resistant to irradiation in vitro. Exp Hematol 18:1002–1007.

Umezawa, A., Maruyama, T., Segawa, K., Shadduck, R.K., Waheed, A. and Hata, J. (1992) Multipotent marrow stromal cell line is able to induce hematopoiesis in vivo. J Cell Physiol 151:197–205.

Umezawa, A., Tachibana, K., Harigaya, K., Kusakari, S., Kato, S., Watanabe, Y. and Takano, T. (1991) Colony-stimulating factor 1 is downregulated during the adipocyte differentiation of H-1/A marrow stromal cells and induced by cachectin/tumor necrosis factor. Mol Cell Biol 11:920–927.

Umezawa, A., Yamamoto, H., Rhodes, K., Klemsz, M.J., Maki, R.A. and Oshima, R.G. (1997) Methylation of an ETS site in the intron enhancer of the keratin 18 gene participates in tissue-specific repression. Mol Cell Biol 17:4885–4894.

Wang, E.A., Rosen, V., D'Alessandro, J.S., Bauduy, M., Cordes, P., Harada, T., Israel, D.I., Hewick, R.M., Kerns, K.M., LaPan, P., et al. (1990) Recombinant human bone morphogenetic protein induces bone formation. Proc Natl Acad Sci USA 87:2220–2224.

Weissman, I.L. (2000) Stem cells: units of development, units of regeneration, and units in evolution. Cell 100:157–168.

Whitlock, C.A. and Witte, O.N. (1982) Long-term culture of B lymphocytes and their precursors from murine bone marrow. Proc Natl Acad Sci USA 79:3608–3612.

Whitlock, C.A. and Witte, O.N. (1987) Long-term culture of murine bone marrow precursors of B lymphocytes. Methods Enzymol 150:275–286.

Zimmerman, L.B., De Jesus-Escobar, J.M. and Harland, R.M. (1996) The Spemann organizer signal noggin binds and inactivates bone morphogenetic protein 4. Cell 86:599–606.

Cardiomyocytes can be generated from marrow stromal cells *in vitro*

Shinji Makino,[1] Keiichi Fukuda,[1] Shunichirou Miyoshi,[1] Fusako Konishi,[1] Hiroaki Kodama,[1] Jing Pan,[1] Motoaki Sano,[1] Toshiyuki Takahashi,[1] Shingo Hori,[1] Hitoshi Abe,[2] Jun-ichi Hata,[2] Akihiro Umezawa,[2] and Satoshi Ogawa[1]

[1]Cardiopulmonary Division, Department of Internal Medicine, and
[2]Department of Pathology, Keio University School of Medicine, Tokyo 160-8582, Japan

Address correspondence to: Keiichi Fukuda, Molecular Cardiology Unit, Cardiopulmonary Division, Department of Internal Medicine, Keio University, 35 Shinanomachi, Shinjuku-ku, Tokyo 160-8582, Japan. Phone: 81-3-3353-1211, ext. 2310; Fax: 81-3-5269-3678; E-mail:kfukuda@mc.med.keio.ac.jp

Received for publication September 21, 1998, and accepted in revised form January 18, 1999.

We have isolated a cardiomyogenic cell line (CMG) from murine bone marrow stromal cells. Stromal cells were immortalized, treated with 5-azacytidine, and spontaneously beating cells were repeatedly screened. The cells showed a fibroblast-like morphology, but the morphology changed after 5-azacytidine treatment in ~30% of the cells; they connected with adjoining cells after one week, formed myotube-like structures, began spontaneously beating after two weeks, and beat synchronously after three weeks. They expressed atrial natriuretic peptide and brain natriuretic peptide and were stained with anti-myosin, anti-desmin, and anti-actinin antibodies. Electron microscopy revealed a cardiomyocyte-like ultrastructure, including typical sarcomeres, a centrally positioned nucleus, and atrial granules. These cells had several types of action potentials, such as sinus node–like and ventricular cell–like action potentials. All cells had a long action potential duration or plateau, a relatively shallow resting membrane potential, and a pacemaker-like late diastolic slow depolarization. Analysis of the isoform of contractile protein genes, such as myosin heavy chain, myosin light chain, and α-actin, indicated that their muscle phenotype was similar to that of fetal ventricular cardiomyocytes. These cells expressed Nkx2.5/Csx, GATA4, TEF-1, and MEF-2C mRNA before 5-azacytidine treatment and expressed MEF-2A and MEF-2D after treatment. This new cell line provides a powerful model for the study of cardiomyocyte differentiation.

J. Clin. Invest. **103**:697–705 (1999)

Introduction

Although significant progress has been made in the molecular understanding of skeletal muscle growth and differentiation (1, 2), little is known about the genes involved in heart development (3). A number of skeletal muscle cell lines have been established (4–6) in which myoblasts can not only regenerate but also differentiate into myotubes. The isolation and extensive characterization of the MyoD gene family were performed using these cell lines (7–9), and these cells have brought significant progress to our molecular understanding of skeletal muscle differentiation (10). The isolation of a cardiomyogenic cell line (CMG) that may facilitate the molecular analysis of cardiomyocyte development has been long awaited (11).

Myocardial infarction is a leading cause of morbidity and mortality in civilized countries. Cardiomyocytes do not regenerate after birth, and they respond to mitotic signals by cell hypertrophy (12, 13) rather than by cell hyperplasia. Loss of cardiomyocytes leads to regional contractile dysfunction, and necrotized cardiomyocytes in infarcted ventricular tissues are progressively replaced by fibroblasts to form scar tissues. Recent studies revealed that transplanted fetal cardiomyocytes could survive in this heart scar tissue (14) and that these transplanted cells limited scar expansion and prevented postinfarction heart failure. The transplantation of cultured cardiomyocytes into the damaged myocardium has been proposed as a future method for the treatment of heart failure (15–17). Although this is a revolutionary idea, it remains infeasible in the clinical setting because it is difficult to obtain donor fetal heart. A CMG cell line could potentially substitute for fetal cardiomyocytes in this therapy. Therefore, both developmental biologists and cardiologists eagerly await the development of a CMG cell line.

Recent reports (18–23) have revealed that marrow stromal cells have many characteristics of mesenchymal stem cells. Pluripotential progenitor marrow stromal cells may differentiate into various types of cell types, including bone (19, 20), muscle (21), fat (22), tendon, or cartilage (23). On the basis of these findings, we hypothesized that marrow stromal cells might also differentiate into cardiomyocytes. We therefore repeatedly screened marrow stromal cells that began spontaneously beating after exposure to 5-azacytidine, a cytosine analog capable of altering expression of certain genes that may regulate differentiation. To our knowledge, this is the first report of the establishment of a cell line that differentiates into cardiomyocytes *in vitro* from adult marrow stromal cells. The cells were characterized electrophysiologically and ultrastructurally and were examined for cardiomyocyte-specific gene expression. The use of adult

Table 1
PCR primers used in this study

	Sense	Anti-sense
ANP	5′-TTGGCTTCCAGGCCATAATTG-3′	5′-AAGAGGGCAGATCTATCGGA-3′
BNP	5′-ATGGATCTCCTGAAGGTGCT-3′	5′-AAGAGGGCAGATCTATCGGA-3′
α-MHC	5′-GGAAGAGTGAGCGGCCATCAAGG-3′	5′-CTGCTGGAGAGGTTATTCCTCG-3′
β-MHC	5′-GCCAACACCAACCTGTCCAAGTTC-3′	5′-TGCAAAGGCTCCAGGTCTGAGGGC-3′
α-skeletal actin	5′-CTCTCTCTCCTCAGGACAA-3′	5′-TGGAGCAAAACAGAATGGCTGG-3′
α-cardiac actin	5′-CTGAGATGTCTCTCTCTCTCTTAG-3′	5′-ACAATGACTGATGAGAGATG-3′
MLC-2a	5′-CAGACCTGAAGGAGACCT-3′	5′-GTCAGCGTAAACAGTTGC-3′
MLC-2v	5′-GCCAAGAAGCGGATAGAAGG-3′	5′-CTGTGGTTCAGGGCTCAGTC-3′
Nkx2.5/Csx	5′-CAGTGGAGCTGGACAAAGCC-3′	5′-TAGCGACGGTTCTGGAACCA-3′
GATA4	5′-CTGTCATCTCACTATGGGCA-3′	5′-CCAAGTCCGAGCAGGAATTT-3′
TEF-1	5′-AAGACGTCAAGCCCTTTGTG-3′	5′-AAAGGAGCACACTTTGGTGG-3′
MEF-2C	5′-AGCAAGAATACGATGCCATC-3′	5′-GAAGGGGTGGTGGTACGGTC-3′
MEF-2D	5′-TGGGAATGGCTATGTCAGTG-3′	5′-CTGGTAATCTGTGTTGTAGG-3′

ANP, atrial natriuretic peptide; *BNP*, brain natriuretic peptide; *MEF*, muscle enhancement factor; *MHC*, myosin heavy chain; *MLC*, myosin light chain.

tissues as a source of cardiomyocytes makes this system particularly appropriate for the development of gene therapy strategies for heart disease.

Methods

Cell culture. Female C3H/He mice (n = 10) were anesthetized with ether, thigh bones were excised, and bone marrow cells were obtained. The procedures were performed in accordance with the guidelines for animal experimentation of Keio University. Primary culture of the marrow cells was performed according to Dexter's method (24). Cells were cultured in Iscove's modified Dulbecco's medium (IMDM) supplemented with 20% FBS and penicillin (100 μg/ml)/streptomycin (250 ng/ml)/amphotericin B (85 μg/ml) at 33°C in humid air with 5% CO_2. After a series of passages, attached marrow stromal cells became homogeneous and were devoid of hematopoietic cells. The marrow stromal cells basically did not require coculture of blood stem cells. Immortalized cells were obtained by frequent subculture for more than 4 months. Cell lines from different dishes were subcloned by limiting dilution. To induce cell differentiation, cells were treated with 3 μmol/l of 5-azacytidine (Sigma Chemical Co., St. Louis, Missouri, USA) for 24 h. Subclones that included spontaneously beating cells were screened by microscopic observation (first screening), and cells surrounding spontaneously beating cells were subcloned by cloning syringes. Subcloned cells were maintained and again exposed to 5-azacytidine for 24 h, and clones that showed spontaneous beating most frequently were screened (second screening). The screened clone was named the CMG (cardiomyogenic) cell.

Videotape recording. The cultured cells were observed through an inverted-type phase-contrast video microscope (TMD300; Nikon, Tokyo, Japan) equipped with a 40× quartz objective lens and an 8× relay lens. The culture dish was kept at 33°C using a temperature-controlled closed chamber. The cell images were introduced into an intensified charged couple device camera (KP-C251; Hitachi Denshi/Sankei, Tokoyo, Japan) and videotaped by an sVHS recorder (VZ-470; Sanyo, Tokyo, Japan). A gray density filter (ND16; Nikon) was used to limit unnecessary light exposure to epi-illumination by a xenon lamp (100 W). Image processing software (NIH Image 1.59/Power Macintosh 7200; National Institutes of Health, Bethesda, Maryland, USA) was used to determine alterations in the size of cells.

Immunostaining. A monoclonal antibody (MF20) to sarcomeric myosin was obtained from American Type Culture Collection (Rockville, Maryland, USA). A monoclonal antibody to desmin was purchased from Bio-Science Products (Emmenbrücke, Switzerland), and a monoclonal antibody to actinin was purchased from Sigma Chemical Co. Cells grown on glass coverslips were permeabilized in 1% formaldehyde/PBS for 10 min. After blocking with 5% BSA in PBS for 1 h at room temperature, the cells were incubated with primary antibodies. After three washes in PBS for 5 min each, the biotinylated/conjugated anti-mouse IgG (DAKO Corp., Carpinteria, California, USA) was applied for 30 min at a dilution of 1:400. Visualization was achieved through the streptavidin-biotin horseradish peroxidase detection system.

Transmission electron microscopy. For transmission electron microscopy of cultured cells, cells were washed three times with PBS (pH 7.4). The initial fixation was done in PBS containing 2.5% glutaraldehyde for 2 h. The cells were embedded in epoxy resin. Ultrathin sections cut horizontally to the growing surface were double stained in uranyl acetate and lead citrate and were viewed under a JEM-1200EX transmission electron microscope (Nihon Denshi, Tokyo, Japan).

Action potential recording. Electrophysiological studies were performed in IMDM containing (in mmol/l) $CaCl_2$ 1.49, KCl 4.23, and HEPES 25 (pH 7.4). Cultured cells were placed on the stage of an inverted phase-contrast optic (Diaphoto-300; Nikon) at room temperature (25°C). Action potentials were recorded by conventional microelectrode. Intracellular recordings were made from 2- to 5-week-old cultured cells with a distinguishable phenotype. Glass microelectrodes filled with KCl (3 mol/l) having a DC resistance of 15–30 MΩ were selected. Membrane potentials were measured by means of current clamp mode (MEZ-8300; Nihon Kohden, Tokyo, Japan) with a built-in four-pole Bessel filter set at 1 kHz. The data were recorded on the thermal recorder (RTA-1100M; Nihon Kohden) and stored on a digital magnetic tape (frequency range 0–20 kHz, Sony Magnescale; Sony Co., Tokyo, Japan) for later analysis.

RNA extraction, reverse transcriptase–PCR, and Southern blot analysis. Total RNA was extracted from adult mouse heart, skeletal muscle, and differentiated CMG cells by Trizol Reagent (GIBCO BRL, Gaithersburg, Maryland, USA). Reverse transcriptase (RT)-PCR of cardiomyocyte-specific genes, including atrial natriuretic peptide (ANP; ref. 25), brain natriuretic peptide (BNP; ref. 26), α- and β-myosin heavy chain (α- and β-MHC; ref. 27), α-skeletal actin, α-cardiac actin, myosin light chain-2a and -2v (MLC-2a and -2v; ref. 28), Nkx2.5/Csx (29, 30), GATA4 (31), TEF-1 (32), MEF-2A, -2C, and -2D (Morisaki, T., personal communication), was performed using 1 μg of total RNA. DNase I was applied at 23°C for 15 min. PCR was performed for 30–35 cycles, with each cycle consist-

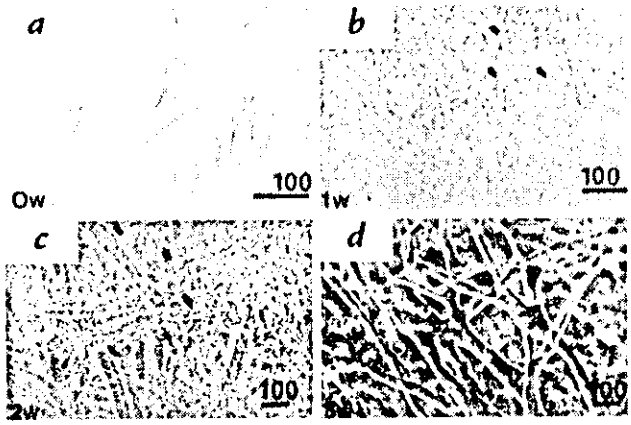

Figure 1
Phase-contrast photographs of CMG cells before and after 5-azacytidine treatment. (*a*) CMG cells show fibroblast-like morphology before 5-azacytidine treatment (0 weeks, *0W*). (*b*) One week after treatment. Some cells gradually increased in size and formed a ball-like or stick-like appearance (*arrowheads*). These cells began spontaneously beating thereafter. (*c*) Two weeks after treatment. Ball-like or stick-like cells connected with adjoining cells and began to form myotube-like structures. (*d*) Three weeks after treatment. Most of the beating cells were connected and formed myotube-like structures. Scale bars: 100 μm. *CMG*, cardiomyogenic cell line.

ing of 95°C for 30 s, 53-60°C for 1.5 min, and 72°C for 1 min, with an additional 7-min incubation at 72°C after completion of the last cycle. The primers used are described in Table 1. The PCR products were size-fractionated by 3% Nu Sieve agarose gel electrophoresis. In some experiments, the gels were transferred to nylon membranes (Hybond N), and ultraviolet cross-linked. The Southern blot hybridization was performed at 42°C for 24 h using a ^{32}P end-labeled internal 25-bp fragment. The internal 25-bp fragments used were as follows: ANP, CTGAGTGAGCAGACTGAGGAAGCAG; BNP, AAAAGTCGGAGGAAATGGCCCAGAG; Nkx2.5 /Csx, TTCAAGCAACAGCGGTACCTGT; GATA4, TGACAGTCATGGGGACATAATCACC; TEF-1, TTGAACAGCAGAGAGACCCAGA. Southern blots were washed several times with a final wash at 55°C in 2× SSC (150 mmol/l NaCl, 15 mmol/l sodium citrate) containing 0.1% SDS for 30 min. After washing, x-ray film was exposed to the filter at -70°C.

Northern blot analysis was used for detection of α-skeletal actin and α-cardiac actin expression. Total RNA (20 μg) was separated on a 1% MOPS/formaldehyde-agarose gel and blotted onto a nylon membrane (Hybond N). cDNAs for α-skeletal actin and α-cardiac actin were obtained by RT-PCR from mouse heart RNA and were cloned into pCR II plasmid. All cDNAs were confirmed by sequencing. Inserts were labeled by random priming with [^{32}P]dCTP (Du Pont NEN Research Products, Boston, Massachusetts, USA). After transfer, the blots were immersed in a Rapid-hyb buffer (Amersham Life Sciences Inc., Arlington Heights, Illinois, USA), and hybridization was performed according to the manufacturer's instructions. Blots were washed serially with a final wash at 55°C-65°C in 0.1× SSC containing 0.1% SDS for 30 min.

Results

CMG cells form myotubes and show spontaneous contraction. We repeated limiting dilutions several times and isolated 192 single clones; however, we observed several clones that could differentiate into the cardiomyocytes and show spontaneous beating. These experiments were repeated and reproducible, but the percentage of cardiomyocyte differentiation was distinct among these clones.

To determine the morphological changes in CMG cells induced by 5-azacytidine treatment, phase-contrast photography and/or immunostaining with anti-sarcomeric myosin, anti-actinin, and anti-desmin antibodies were performed on CMG cells. Figure 1 is a phase-contrast photograph of CMG cells before and after 5-azacytidine treatment. CMG cells showed a fibroblast-like morphology before 5-azacytidine treatment (0 week), and this phenotype was retained through repeated subcultures under nonstimulating conditions. After 5-azacytidine treatment, the morphology of the cells gradually changed. Approximately 30% of the CMG cells gradually increased in size, formed a ball-like appearance, or lengthened in one direction and formed a stick-like morphology at one week. They connected with adjoining cells after two weeks and formed myotube-like structures at three weeks. After the CMG cells differentiated to the cardiomyocytes, they could divide in culture to some extent. The differentiated CMG myotubes maintained cardiomyocyte phenotype and beat vigorously for at least eight weeks after final 5-azacytidine treatment, and they did not dedifferentiate. Most of the other nonmyocytes showed an adipocyte-like appearance.

Figure 2 shows the immunostaining of the CMG cells with anti-sarcomeric myosin antibody (MF20) at one, two, three, and four weeks after 5-azacytidine treatment. Myosin-positive cells gradually joined with neighboring myosin-positive cells and formed a myotube-like appearance. The maximum length of the myotubes ranged from 1,000 μm to 3,000 μm. Cardiac muscle cells can be distinguished from skeletal muscle cells by the presence of branching fibers, and the CMG myotubes showed a number of branches. Figure 3 shows high magnification of the immunostaining of the differentiated CMG myotubes at four weeks with anti-myosin, anti-actinin, and anti-desmin antibodies. Most of the cells were

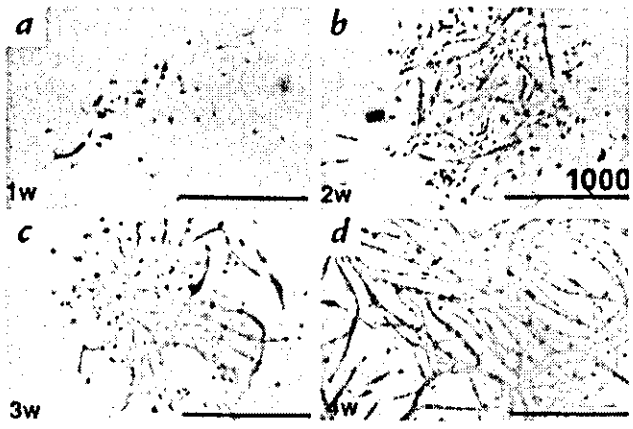

Figure 2
Immunostaining of CMG cells with anti-sarcomeric myosin antibody at 1 week (*a*), 2 weeks (*b*), 3 weeks (*c*), and 4 weeks (*d*) after 5-azacytidine treatment. Myosin-positive cells could be observed at 1 week after 5-azacytidine treatment. Myosin-positive cells gradually joined to neighboring myosin-positive cells and formed myotube-like structures. Scale bars: 1,000 μm. The maximal length of the myotube was 3,000 μm.

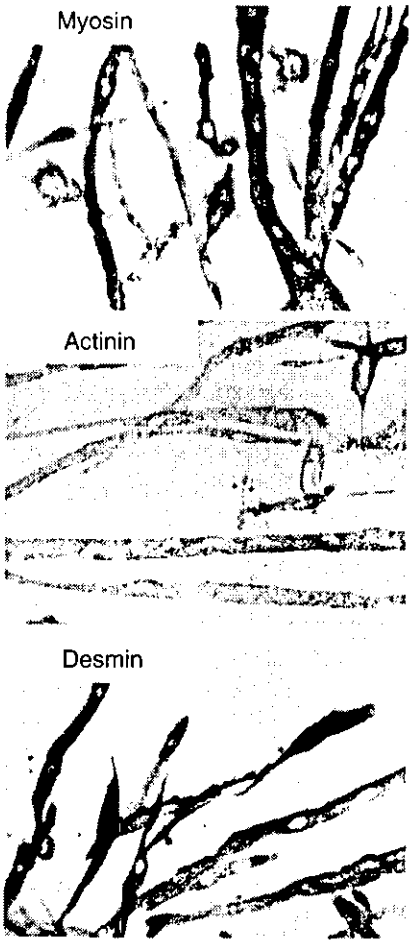

Figure 3
Immunostaining of CMG cells with anti-sarcomeric myosin, anti-actinin, and anti-desmin antibodies after 5-azacytidine treatment (3 weeks). CMG myotubes were stained with both anti-sarcomeric myosin, anti-actinin, and anti-desmin antibodies.

mononuclear, some were binuclear, but a few were multinucleated (3-10 per cell). Cells were connected to each other via intercalated discs and formed myotubes. CMG myotubes also stained strongly with anti-actinin and anti-desmin antibodies.

Figure 4 shows sequential photographs of the CMG myotubes obtained from a videotape recording that represents one contraction. Differentiated CMG myotubes showed repeated spontaneous contraction and relaxation without any stimulation. Spontaneous beating was also observed in isolated CMG cells. Myotubes began spontaneously beating after two weeks and beat synchronously after three weeks. The contractions were rapid and automatic—very different from those of smooth muscle cells and skeletal muscle cells in culture. The frequency of contractions ranged from 63 to 428 per minute.

CMG cells have a cardiomyocyte-like ultrastructure. Representative transmission electron microscopy photographs are shown in Fig. 5. Immature CMG cells at one to two weeks after treatment showed myofilaments, but their alignment was intricate (data not shown). However, a longitudinal section of the differentiated CMG myotubes clearly revealed the typical striation and pale-staining pattern of the sarcomeres (Fig. 5*a*). CMG myotube nuclei were positioned in the center of the cell, not beneath the sarcolemma. The most conspicuous feature of the differentiated CMG myotubes was the presence of membrane-bound dense secretory granules measuring 70-130 nm in diameter (Fig. 5*b*). These granules were thought to be atrial granules and were especially concentrated in the juxtanuclear cytoplasm, but some were also located near the sarcolemma. These findings indicated that CMG cells had a cardiomyocyte-like, rather than skeletal muscle, ultrastructure.

CMG myotubes have several types of action potential. An electrophysiological study was performed on differentiated CMG cells at two to five weeks after 5-azacytidine treatment. There were at least two types of distinguishable morphological action potentials: sinus node-like potentials (Fig. 6*a*) and ventricular myocyte-like potentials (Fig. 6*b*). The sinus node-like action potential showed a relative shallow resting membrane potential with late diastolic slow depolarization, like a pacemaker potential. Peak- and domelike morphology were observed in ventricular myocyte-like cells. Table 2 gives the action potentials recorded in CMG myotubes. A cardiomyocyte-like action potential recorded from these spontaneously beating cells had the following properties: (*a*) a relatively long action potential duration or plateau (*b*) a relatively shallow resting membrane potential, and (*c*) a pacemaker-like late diastolic slow depolarization. Figure 7 shows a time course of the percentage of the sinus node-like and ventricular myocyte-like action potentials of the CMG cells after 5-azacytidine treatment. All the action potentials recorded from the CMG cells until three weeks revealed sinus node-like action potential. The ventricular myocyte-like action potentials could be recorded after four weeks, and the percentage of these action potentials gradually increased thereafter. It is possible that the percentage of the ventricular myocyte-like action potentials at five weeks was underestimated. Most of the action potentials recorded from differentiated CMG myotubes revealed ventricular myocyte-like appearance, but the action potential of the differentiated CMG myotubes was difficult to record. The glass microelectrode was frequently damaged because the spontaneous contraction of the differentiated myotube at five weeks was too big.

Cardiomyocyte-specific gene expression. Figure 8 shows RT-PCR or Northern blot analysis of the expression of cardiomyocyte-specific genes in differentiated CMG cells. Figure 7*a* represents an RT-PCR Southern blot using ANP and BNP gene probes. Total RNA obtained from

Table 2
Measurement of action potentials recorded in CMG myotubes

	BCL (ms)	APD (ms)	MDP (mV)	APA (mV)	*n*
Sinus node-like cell	143-788	46.6 ± 15.5	-54.8 ± 9.4	58.5 ± 14.6	40
Ventricular-like cell	108-950	58.2 ± 14.1	-59.5 ± 7.8	71.0 ± 13.2	18

APA, action potential amplitude; *APD*, action potential duration; *BCL*, beating cycle length; *MDP*, most diastolic membrane potential.

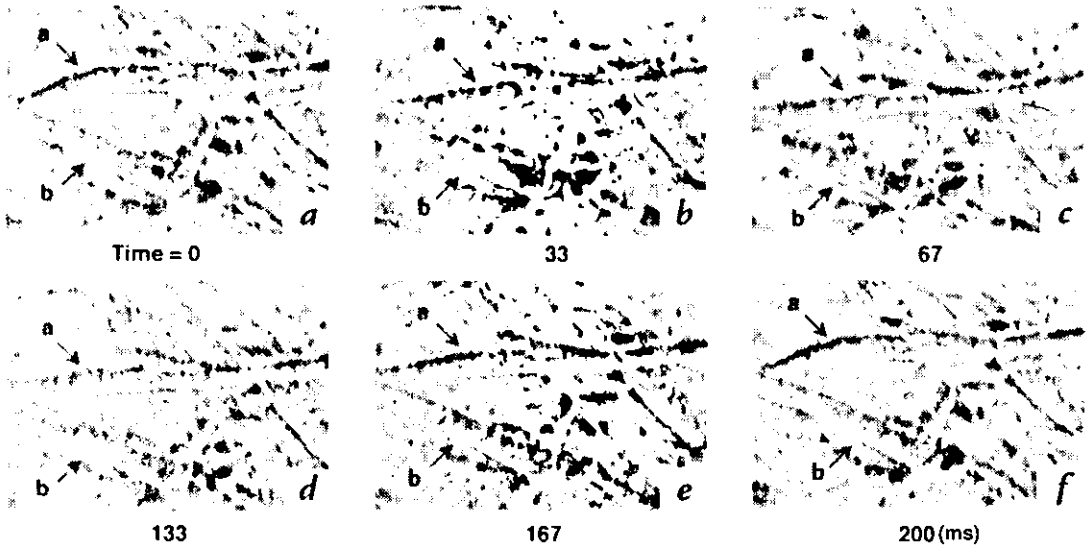

Figure 4
A series of photographs representing one contraction of beating CMG myotubes recorded by phase-contrast video microscope. The beating differentiated CMG myotubes were videotaped as described in Methods. In each panel, *a* and *b* represent branches of a single myotube that beat spontaneously. Panel *a* is at the end of relaxation and panel *b* is at maximum contraction.

cardiomyocytes (*in vivo* heart) and skeletal muscles (soleus muscle) were used as positive and negative controls, respectively. Differentiated CMG myotubes expressed both the ANP and BNP genes. Figure 8*b* shows the expression of the α- and β-MHC, α-cardiac and α-skeletal actin genes. Both α- and β-MHC expression could be detected by RT-PCR in differentiated CMG cells, but β-MHC expression was overwhelmingly stronger than that of α-MHC. CMG cells expressed both α-cardiac and α-skeletal actin. Figure 8*c* shows the Northern blot analysis of α-cardiac and α-skeletal actin gene expression. Adult mouse heart was used as a positive control. The α-skeletal actin gene was expressed at markedly higher levels than the α-cardiac actin gene in CMG cells. Interestingly, CMG cells expressed MLC-2v, but not MLC-2a (Fig. 8*d*).

Figure 9 shows the expression of cardiomyocyte-specific transcription factors. Figure 9*a* represents the RT-PCR–Southern blot analysis of Nkx2.5/Csx, GATA4, and TEF-1 in CMG cells. Cardiomyocytes expressed GATA4, TEF-1, and Nkx2.5/Csx, whereas skeletal muscle cells only expressed TEF-1. Differentiated CMG myotubes expressed GATA4, TEF-1, and Nkx2.5/Csx. Figure 9*b* represents the time course of GATA4, TEF-1, and Nkx2.5/Csx gene expressions in CMG cells. Interestingly, CMG cells already expressed these genes before 5-azacytidine treatment. Figure 9*c* shows the time course of MEF-2A, MEF-2C, and MEF-2D gene expression. Because the primers were designed to demonstrate the alternative splicing forms of MEF-2 genes, several bands could be observed. MEF-2C was already expressed before 5-azacytidine treatment, but MEF-2A and MEF-2D were induced after 5-azacytidine treatment.

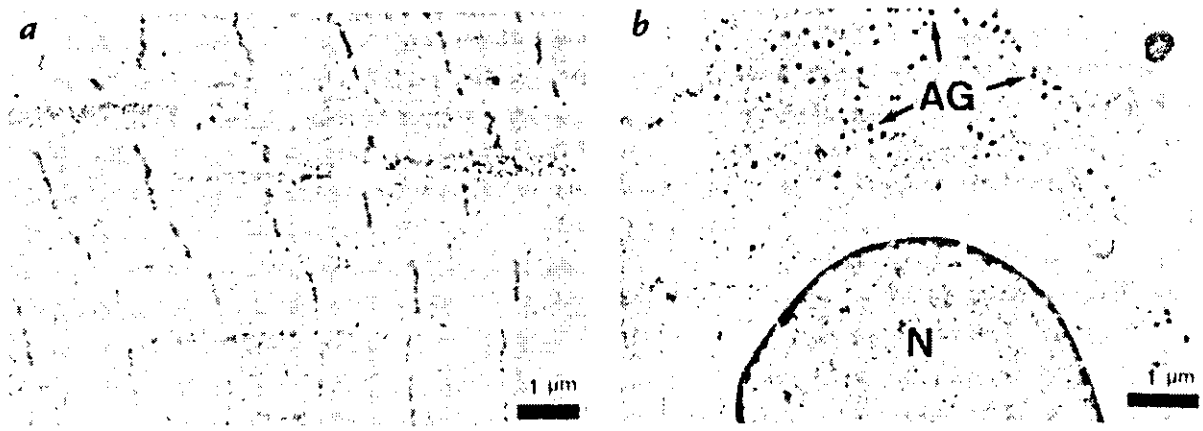

Figure 5
Transmission electron micrograph of CMG myotubes. (*a*) Differentiated CMG myotubes revealed well-organized sarcomeres. Rich glycogen granules and a number of mitochondria were observed. (*b*) Ultrastructural analysis revealed that nuclei (*N*) were oval and positioned in the central part of the cell, not immediately beneath the sarcolemma. Atrial granules (*AG*), measuring 70–130 nm in diameter, are observed in the sarcoplasm and are concentrated especially in the juxtanuclear cytoplasm. Scale bars: 1 μm.

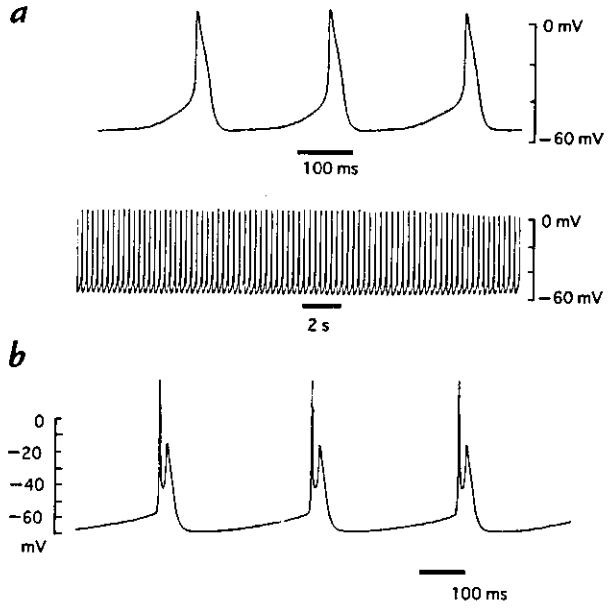

Figure 6
Representative tracing of the action potential of CMG myotubes. Action potential recordings using a conventional microelectrode were obtained from the spontaneously beating cells at day 28 after 5-azacytidine treatment. We categorized these action potentials into two groups: a sinus node-like action potential (*a*) or a ventricular cardiomyocyte-like action potential (*b*). These action potentials have a relatively shallow resting membrane potential with late diastolic slow depolarization: a pacemaker-like potential. The ventricular cardiomyocyte-like action potential had peak notch-plateau characteristics, with an initial tall overshoot in phase 0, a repolarizing notch in phase 1, and a second depolarizing plateau in phase 2, whereas the sinus node-like action potential had none of these features. Beating cycle length, action potential amplitude, action potential duration, and most diastolic potential are given in Table 2.

Discussion

We have established a cardiomyogenic cell line (CMG) from mouse bone marrow stromal cells that can be induced to differentiate into cardiomyocytes *in vitro* by 5-azacytidine treatment. A number of lines of evidence confirmed the cardiomyocyte characteristics of CMG cells. These cells expressed a number of cardiomyocyte-specific genes including ANP, BNP, GATA4, and Nkx2.5/Csx. In ventricular muscle of small mammals, there is a developmental switch from expression of β-MHC, which is the predominant fetal form, to that of α-MHC around the time of birth. There is also a developmental switch from expression of α-skeletal actin, which is the predominant fetal and neonatal form, to that of α-cardiac actin, the predominant adult form. Differentiated CMG cells mainly expressed β-MHC and α-skeletal actin. Expression of α-MHC and α-cardiac actin was detected, but at low levels. MLC-2 genes are specifically expressed in the chamber. MLC-2v is specifically expressed in ventricular cells, whereas MLC-2a was specifically expressed in atrial cells. Differentiated CMG cells expressed MLC-2v, but not MLC-2a. Moreover, skeletal muscle cells do not express α-MHC or MLC-2v. These results indicated that differentiated CMG cells had a phenotype specific to fetal ventricular cardiomyocytes.

Differentiated CMG cells expressed Nkx2.5/Csx, GATA4, TEF-1, and MEF-2C before final 5-azacytidine treatment. The MEF-2A and MEF-2D genes were expressed after final 5-azacytidine treatment. This pattern of gene expression in CMG cells was similar to that of *in vivo* developing cardiomyocytes (33). These results indicate that the stage of differentiation of the CMG cell is between cardiomyocyte-progenitor and differentiated cardiomyocytes.

Differentiated CMG cells connected to adjoining cells via intercalated discs, formed myotubes, and beat spontaneously. These differentiated CMG myotubes have a cardiomyocyte-like ultrastructure, including typical sarcomeres, a centrally positioned nucleus, abundant glycogen granules, a number of mitochondria, and many atrial granules. Tagoe *et al.* (34) reported that the most common size of atrial granules observed in the adult mice atrium was 150–200 nm in diameter, but they also found that ~35% of the atrial granules in adult mice atria ranged between 50 and 150 nm in diameter. The atrial granules observed in the differentiated CMG myotubes were 70–130 nm in diameter. A previous report (35) found that almost all atrial myocytes expressed ANP in fetal heart, whereas in the ventricular wall, cells containing immunoreactive granules were scattered. Analysis of the pattern of expression of cardiomyocyte-specific genes indicated that the phenotype of the differentiated CMG cardiomyocytes corresponded to fetal ventricular cardiomyocytes. The high-density granules observed in the differentiated CMG cells might correspond to those in fetal ventricular cardiomyocytes.

CMG myotubes have either sinus node-like or ventricular myocyte-like action potentials with a relatively long action potential duration or plateau, a relatively shallow resting membrane potential, and a pacemaker-like late diastolic slow depolarization.

Although action potentials can be seen in noncardiomyocyte cells such as skeletal muscle cells or nerve cells, the action potential in CMG cells is characterized by duration (36–39). The duration of action potentials in

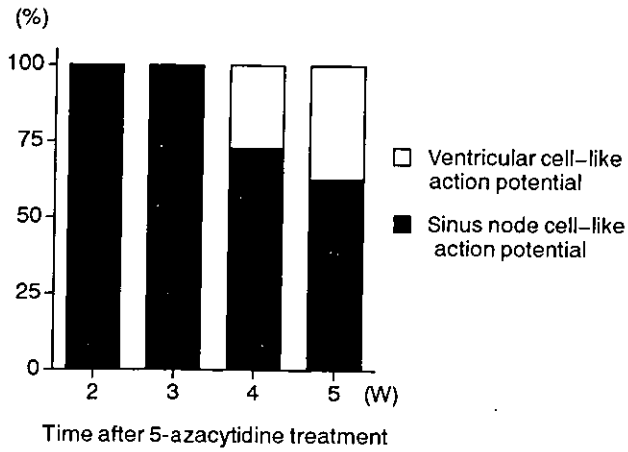

Figure 7
Time course of the percentage of the pattern of action potentials in CMG myotubes. The percentage of the sinus node-like and ventricular cardiomyocyte-like action potential of the CMG cells after 5-azacytidine treatment was demonstrated. Ventricular cardiomyocyte-like action potential was first recorded 4 weeks after 5-azacytidine treatment, and incidence rapidly increased thereafter.

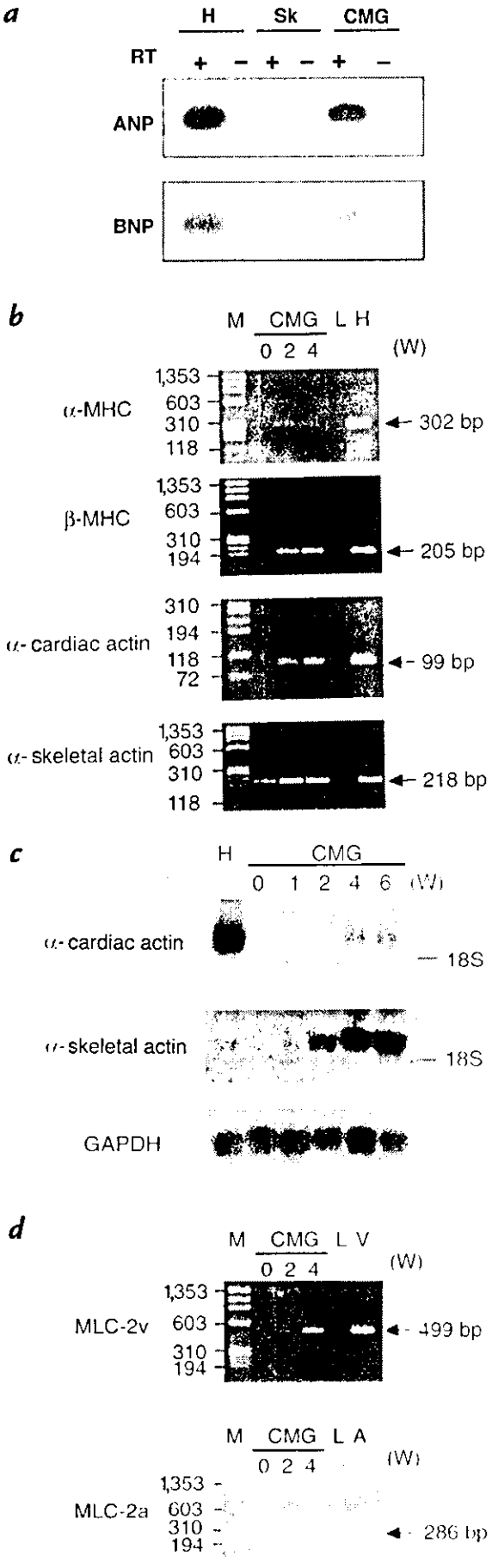

Figure 8

Expression of cardiomyocyte-specific genes in and phenotype analysis of CMG cells. (*a*) reverse transcriptase (*RT*)-PCR Southern analysis of natriuretic peptide (*ANP*) and brain natriuretic peptide (*BNP*) in CMG cells. Total RNA was isolated from mouse heart (*H*), skeletal muscle (*Sk*), and differentiated CMG cells. After DNase I treatment, RT-PCR was performed, as described in Methods, for ANP and BNP. Each PCR product was identified by Southern blot using ^{32}P-labeled synthetic oligonucleotides. Both ANP and BNP are specifically expressed in cardiac muscle and CMG myotubes. (*b*) RT-PCR analysis of α-myosin heavy chain (*α-MHC*), β-myosin heavy chain (*β-MHC*), α-cardiac actin, and α-skeletal actin expression in CMG cells. Heart (*H*) and liver (*L*) were used as positive and negative controls. *M* represents Φ*X*174*Hae*III molecular size marker. CMG myotubes expressed both α-cardiac actin and α-skeletal actin, but the expression of α-skeletal actin was much stronger than that of α-cardiac actin. Note that α-skeletal actin expression was observed before the final 5-azacytidine treatment, although expression was weak. CMG myotubes expressed both α- and β-MHC, but the expression of β-MHC was much stronger than that of α-MHC. (*c*) Northern blot analysis of α-cardiac actin and α-skeletal actin expression in CMG cells. Adult heart (*H*) was used as a positive control. α-cardiac actin was more abundantly expressed in adult heart. On the other hand, α-skeletal actin was more abundantly expressed in CMG cells. Glyceraldehyde-3-phosphate dehydrogenase (*GAPDH*) was used as a loading internal control. (*d*) RT-PCR analysis of MLC-2a and -2v expression in CMG cells. Adult atrial muscle (*A*) was used as a positive control for MLC-2a, and adult ventricular muscle (*V*) was used as a positive control for MLC-2v. *M* represents Φ*X*174*Hae*III molecular size marker. CMG myotubes expressed MLC-2v, but not MLC-2a. These patterns of gene expression in the CMG myotubes corresponded to the phenotype specific to fetal ventricular cardiomyocytes.

skeletal muscle cells or nerve cells are <5 ms (40, 41). The most diastolic potential, action potential amplitude, and the overshoot potential of the sinus node-like CMG cells were close to the equivalent values reported *in vivo* rabbit sinus node cells (42). In rabbit ventricular cells, the most diastolic potential and action potential amplitude were reported to be approximately between -90 and -95mV, and 120 mV, respectively. Although the most diastolic potential and action potential amplitude of the ventricular cardiomyocyte-like CMG cells were slightly shorter than these values, the shape of the action potential was very close to *in vivo* ventricular cardiomyocyte. The observation of several distinctive patterns of action potential in CMG cells may reflect different developmental stages. The electrophysiological patterns of action potential and expression patterns of the ion channels in differentiated CMG cells should be clarified in the future.

Both embryonic stem (ES) cells (43) and embryonal carcinoma (EC) cells (44, 45) may differentiate into cardiomyocytes *in vitro*. These cells were derived from totipotent embryonal blastocyst and either required endoderm for mesodermal differentiation or could differentiate into endoderm and ectoderm by themselves. CMG cells differ from these cells in several ways. First, CMG cells were obtained from adult bone marrow. Second, they did not require endoderm for differentiation, and they only differentiated into mesoderm, as demonstrated in other marrow stromal cell lines. Third, CMG cells were easy to culture because they are adherent like fibroblasts, have a high growth rate, and do not require expensive cytokine (leukemia inhibitory factor) supplement. Finally, differentiation is easily induced by 5-azacytidine treatment. ES cells

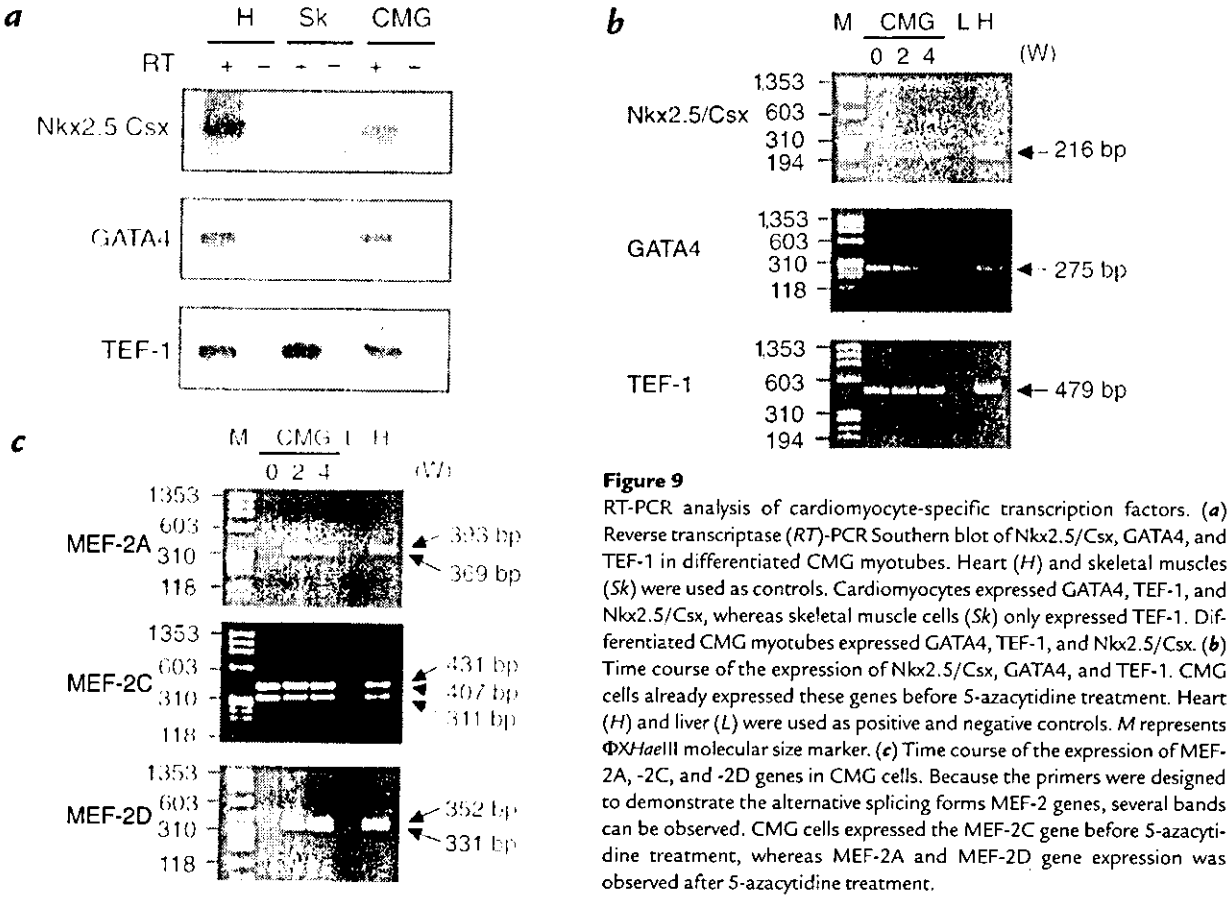

Figure 9

RT-PCR analysis of cardiomyocyte-specific transcription factors. (*a*) Reverse transcriptase (*RT*)-PCR Southern blot of Nkx2.5/Csx, GATA4, and TEF-1 in differentiated CMG myotubes. Heart (*H*) and skeletal muscles (*Sk*) were used as controls. Cardiomyocytes expressed GATA4, TEF-1, and Nkx2.5/Csx, whereas skeletal muscle cells (*Sk*) only expressed TEF-1. Differentiated CMG myotubes expressed GATA4, TEF-1, and Nkx2.5/Csx. (*b*) Time course of the expression of Nkx2.5/Csx, GATA4, and TEF-1. CMG cells already expressed these genes before 5-azacytidine treatment. Heart (*H*) and liver (*L*) were used as positive and negative controls. *M* represents ΦX*Hae*III molecular size marker. (*c*) Time course of the expression of MEF-2A, -2C, and -2D genes in CMG cells. Because the primers were designed to demonstrate the alternative splicing forms MEF-2 genes, several bands can be observed. CMG cells expressed the MEF-2C gene before 5-azacytidine treatment, whereas MEF-2A and MEF-2D gene expression was observed after 5-azacytidine treatment.

and EC cells differentiate into cardiomyocytes at rates of ~50% and 5%, respectively. CMG cells differentiate into cardiomyocyte-like cells after final 5-azacytidine treatment, and the efficiency of the differentiation into cardiomyocytes is ~30%. Thus, CMG cells provide a powerful tool for the further investigation of cardiomyocyte differentiation. Although transcription factors such as d-HAND, e-HAND (46), MEF-2C (33, 47), Nkx2.5/Csx, GATA4, and TEF-1 are known to play important roles in cardiac development (48), the lack of a model for cardiomyocyte differentiation has meant that little is known about the interactions of these genes. This simple new model for cardiomyogenesis may help clarify the cascade of transcriptional activation that regulates differentiation into cardiomyocytes.

Acknowledgments

We thank Makoto Suematsu for help with video recording of CMG myotube contraction and Naomichi Yagi for the ultrastructural examination. The authors also acknowledge Yoshiko Kurokawa and Rie Inaba for technical assistance. This study was supported in part by research grants of "Research for the Future" Program from the Japan Society for the Promotion of Science (JSPS-RFTF97I00201); the Ministry of Education, Science and Culture of Japan; the Ministry of Welfare of Japan; and the Japan Owner's Association.

1. Weintraub, H. 1993. The MyoD family and myogenesis: redundancy, networks, and thresholds. *Cell.* **75**:1241-1244.
2. Silberstein, L., Webster, S.G., Travis, M., and Blau, H.M. 1986. Developmental progression of myosin gene expression in cultured muscle cells. *Cell.* **46**:1075-1081.
3. Olson, E.N., and Srivastava, D. 1996. Molecular pathways controlling heart development. *Science.* **272**:671-676.
4. Lassar, A.B., Paterson, B.M., and Weintraub, H. 1986. Transfection of a DNA locus that mediates the conversion of 10T1/2 fibroblasts to myoblasts. *Cell.* **47**:649-656.
5. Taylor, S.M., and Jones, P.A. 1979. Multiple new phenotypes induced in 10T1/2 and 3T3 cells treated with 5-azacytidine. *Cell.* **17**:771-779.
6. Murry, C.E., Wiseman, R.W., Schwartz, S.M., and Hauschka., S.D. 1996. Skeletal myoblast transplantation for repair of myocardial necrosis. *J. Clin. Invest.* **98**:2512-2523.
7. Rhodes, S.J., and Konieczny, S.F. 1989. Identification of MRF4: a new member of the muscle regulatory factor gene family. *Genes Dev.* **3**:2050-2061.
8. Wright, W.E., Sassoon, D.A., and Lin, V.K. 1989. Myogenin, a factor regulating myogenesis, has a domain homologous to MyoD. *Cell.* **56**:607-617.
9. Braun, T., Winter, B., Bober, E., and Arnold, H.H. 1990. Transcriptional activation domain of the muscle-specific gene-regulatory protein myf5. *Nature.* **346**:663-665.
10. Rawls, A., and Olson, E.N. 1997. MyoD meets its maker. *Cell.* **89**:5-8.
11. Fishman, M.C., and Chien, K.R. 1997. Fashioning the vertebrate heart: earliest embryonic decisions. *Development.* **124**:2099-2117.
12. Kodama, H., *et al.* 1997. Leukemia inhibitory factor, a potent cardiac hypertrophic cytokine, activates the JAK/STAT pathway in rat cardiomyocytes. *Circ. Res.* **81**:656-663.
13. Pan, J., *et al.* 1997. Role of angiotensin II in activation of the JAK/STAT pathway induced by acute pressure overload in the rat heart. *Circ. Res.* **81**:611-617.
14. Leor, J., Patterson, M., Quinones, M.J., Kedes, L.H., and Kloner, R.A. 1996. Transplantation of fetal myocardial tissue into the infarcted myocardium of rat. A potential method for repair of infarcted myocardium? *Circulation.* **94**(Suppl. II):332-336.
15. Li, R.K., *et al.* 1997. Natural history of fetal rat cardiomyocytes transplanted into adult rat myocardial scar tissue. *Circulation.* **96**(Suppl. II):179-186.
16. Soonpaa, M.H., Koh, G.Y., Klug, M.G., and Field, L.J. 1994. Formation of nascent intercalated disks between grafted fetal cardiomyocytes and host myocardium. *Science.* **264**:98-101.
17. Delcarpio, J.B., and Claycomb, W.C. 1995. Cardiomyocyte transfer into

the mammalian heart. Cell-to-cell interactions *in vivo* and *in vitro*. *Ann. NY Acad. Sci.* **752**:267–285.
18. Prockop, D.J. 1997. Marrow stromal cells as stem cells for nonhematopoietic tissues. *Science.* **276**:71–74.
19. Rickard, D.J., Sullivan, T.A., Shenker, B.J., Leboy, P.S., and Kazhdan, I. 1994. Induction of rapid osteoblast differentiation in rat bone marrow stromal cell cultures by dexamethasone and BMP-2. *Dev. Biol.* **161**:218–228.
20. Friedenstein, A.J., Chailakhyan, R.K., and Gerasimov, U.V. 1987. Bone marrow osteogenic stem cells: *in vitro* cultivation and transplantation in diffusion chambers. *Cell Tissue Kinet.* **20**:263–272.
21. Ferrari, G., *et al.* 1998. Muscle regeneration by bone marrow-derived myogenic progenitors. *Science.* **279**:1528–1530.
22. Umezawa, A., *et al.* 1992. Multipotent marrow stromal cell line is able to induce hematopoiesis *in vivo*. *J. Cell. Physiol.* **151**:197–205.
23. Ashton, B.A., *et al.* 1980. Formation of bone and cartilage by marrow stromal cells in diffusion chambers *in vivo*. *Clin. Orthop.* **151**:294–307.
24. Dexter, T.M., Allen, T.D., and Lajtha, L.G. 1977. Conditions controlling the proliferation of haemopoietic stem cells *in vitro*. *J. Cell Physiol.* **91**:335–344.
25. Seidman, C.E., Bloch, K.D., Klein, K.A., Smith, J.A., and Seidman, J.G. 1984. Nucleotide sequences of the human and mouse atrial natriuretic factor genes. *Science.* **226**:1206–1209.
26. Sudoh, T., Kangawa, K., Minamino, N., and Matsuo, H. 1988. A new natriuretic peptide in porcine brain. *Nature.* **332**:78–81.
27. Robbins, J., Gulick, J., Sanchez, A., Howles, P., and Doetschman, T. 1990. Mouse embryonic stem cells express the cardiac myosin heavy chain genes during development *in vitro*. *J. Biol. Chem.* **265**:11905–11909.
28 Kubalak, S.W., Miller-Hance, W.C., O'Brien, T.X., Dyson, E., and Chien, K.R. 1994. Chamber specification of atrial myosin light chain-2 expression precedes septation during murine cardiogenesis. *J. Biol. Chem.* **269**:16961–16970.
29. Komuro, I., and Izumo, S. 1993. Csx: a murine homeobox-containing gene specifically expressed in the developing heart. *Proc. Natl. Acad. Sci. USA.* **90**:8145–8149.
30. Lints, T.J., Parsons, L.M., Hartley, L., Lyons, I., and Harvey, R.P. 1993. Nkx-2.5: a novel murine homeobox gene expressed in early heart progenitor cells and their myogenic descendants. *Development.* **119**:419–431.
31. Arceci, R.J., King, A.A., Simon, M.C., Orkin, S.H., and Wilson, D.B. 1993. Mouse GATA-4: a retinoic acid-inducible GATA-binding transcription factor expressed in endodermally derived tissues and heart. *Mol. Cell. Biol.* **13**:2235–2246.
32. Chen, Z., Friedrich, G.A., and Soriano, P. 1994. Transcriptional enhancer factor 1 disruption by a retroviral gene trap leads to heart defects and embryonic lethality in mice. *Genes Dev.* **8**:2293–2301.
33. Edmondson, D.G., Lyons, G.E., Martin, J.F., and Olson, E.N. 1994. Mef2 gene expression marks the cardiac and skeletal muscle lineages during mouse embryogenesis. *Development.* **120**:1251–1263.
34. Tagoe, C.N., Ayettey, A.S., and Yates, R.D. 1993. Comparative ultrastructural morphometric analysis of atrial specific granules in the bat, mouse, and rat. *Anat. Rec.* **235**:87–94.
35. Venance, S.L., and Pang, S.C. 1989. Ultrastructure of atrial and ventricular myocytes of newborn rats: evidence for the existence of specific atrial granule-like organelles in the ventricle. *Histol. Histopathol.* **4**:325–333.
36. Irisawa, H. 1989. Electrophysiology and contractile function. In *Isolated adult cardiomyocytes.* H.M. Piper and G. Isenberg, editors. CRC Press. Boca Raton, FL. 1–11.
37. Hoffman, B.F., and Cranefield, P.F. 1976. *Electrophysiology of the heart.* McGraw-Hill. New York, NY. 75–131.
38. Carmeliet, E. 1978. Cardiac transmembrane potentials and metabolism. *Circ. Res.* **42**:577–587.
39. Draper, M.H., and Weidman, S. 1951. Cardiac resting and action potentials recorded with an intracellular electrode. *J. Physiol.* **115**:74–94.
40. Nicholls, J.G., Martin, A.R., and Wallace, B.G. 1992. In *From neuron to brain: a cellular and molecular approach to the function of the nervous system.* 3rd ed. J.G. Nicholls, A.R. Martin, and B.G. Wallace, editors. Sinauer Associates. Sunderland, MA. 90–120.
41. Brinley, F.J., Jr. 1980. Excitation and conduction in nerve fibers. In *Medical physiology.* 14th ed. V.B. Mountcastle, *et al.*, editors. Mosby. St. Louis, MO. 46–81.
42. Noma, A., and Irisawa, H. 1976. Membrane currents in the rabbit sinoatrial node cell as studied by the double microelectrode method. *Pflugers Arch.* **364**:45–52.
43. Doetschman, T.C., Eistetter, H., Katz, M., Schmidt, W., and Kemler, R. 1985. The *in vitro* development of blastocyst-derived embryonic stem cell lines: formation of visceral yolk sac, blood islands and myocardium. *J. Embryol. Exp. Morphol.* **87**:27–45.
44. McBurney, M.W., Jones-Villeneuve, E.M., Edwards, M.K., and Anderson, P.J. 1982. Control of muscle and neuronal differentiation in a cultured embryonal carcinoma cell line. *Nature.* **299**:165–167.
45. Jones-Villeneuve, E.M., McBurney, M.W., Rogers, K.A., and Kalnins, V.I. 1982. Retinoic acid induces embryonal carcinoma cells to differentiate into neurons and glial cells. *J. Cell Biol.* **94**:253–262.
46. Srivastava, D., Cserjesi, P., and Olson, E.N. 1995. A subclass of bHLH proteins required for cardiac morphogenesis. *Cell.* **56**:607–617.
47. Lin, Q., Schwarz, J., Bucana, C., and Olson, E.N. 1997. Control of mouse cardiac morphogenesis and myogenesis by transcription factor MEF2C. *Science.* **276**:1404–1407.
48. Harvey, R.P. 1996. NK-2 homeobox genes and heart development. *Dev. Biol.* **178**:203–216.

Pathology International 1996; **46**: 243–252

Original Article

Expression of bone marrow stromal cell specific antigen during murine development: Its expression in embryonic hematopoietic tissues as well as in other developing tissues

Yoshikiyo Akasaka,[1,2] Akihiro Umezawa,[2] Hiroshi Suzuki,[2] Tetsuro Sugimoto[2,3] and Jun-ichi Hata[2]

[1]Second Department of Pathology, Toho University School of Medicine, Tokyo, [2]Department of Pathology, Keio University School of Medicine, Tokyo and [3]Toxicology Research Laboratories, Chugai Pharmaceutical Co., Ltd, Nagano, Japan

Monoclonal antibody R4-A9 demonstrated specificity for a cell surface antigen of stromal cells in murine bone marrow and spleen. In order to identify patterns of expression that may elucidate the potential role of R4-A9 antigen, the developmental expression of this antigen in mouse embryos from 8 days post-coitum to 5 days post-partum was investigated by immunohistochemistry. At an early developmental stage, weak staining for R4-A9 antigen could be detected in the yolk sac. At later stages, strong staining of this antigen was detected predominantly in the embryonic liver, the main site of embryonic hematopoiesis. However, concomitant with the decreased staining in the liver, increased expression of this antigen was observed in bone marrow and spleen. Therefore, the changes in expression in those hematopoietic tissues suggest that its expression is coordinately regulated during the developmental stage of the sites of embryonic hematopoiesis. Compared with the distribution of R4-A9 antigen in adult tissues as previously reported, the expression of this antigen in fetal tissues was more widespread during the period of organogenesis, and was most abundant in other developing tissues, including the heart, skin, and lung. In contrast, fetal expression detected in hematopoietic and other developing tissues was lost after birth. These results taken together show a marked gradient of R4-A9 antigen expression, with the highest level at the peak of organ development, raising the possibility that this molecule may act as a growth/differentiation factor both in hematopoietic and other developing tissues in a fetus.

Key words: bone marrow stromal cell, embryonic development, immunohistochemistry, monoclonal antibody

Correspondence: Yoshikiyo Akasaka, MD, Second Department of Pathology, Toho University School of Medicine, 5-21-16 Omori-nishi, Ohta-ku, Tokyo 143, Japan.

Received 31 August 1995. Accepted for publication 21 December 1995.

The hematopoietic microenvironment plays a critical role in the proliferation and differentiation of hematopoietic stem cells.[1-3] While the detailed mechanisms involved in determining hematopoietic stem cell behavior are not fully known, surface molecules of stromal cells probably play an important role in mediating cellular differentiation through the direct contact of hematopoietic stem cells with stromal cells.[4-8] However, the precise role of stromal cell surface molecules that participate in the interaction between stromal cells and hematopoietic cells is not fully known.[3] To deal with this issue in detail, we attempted to produce a monoclonal antibody against a cell surface antigen of bone marrow stromal cells. We have established a rat monoclonal antibody, designated R4-A9, which recognizes a cell surface antigen of murine bone marrow stromal cells *in vivo* as well as *in vitro*.[9]

In the staining of various tissues, R4-A9 demonstrated specificity for hematopoietic stroma both in bone marrow and spleen. No staining was observed in the thymus, lymph nodes or other tissues, with the exception of Leydig cells in the testis and endothelial cells in small arteries in several organs.[9] These results suggested that the R4-A9 antigen may be a novel molecule that is selectively expressed on the surface of hematopoietic stromal cells. However, it is uncertain whether the R4-A9 antigen functions, for example, in the role played by stromal cells in the hematopoietic microenvironment. In order to gain an insight into the physiological function of the R4-A9 antigen, we have undertaken to obtain further information on the functional role of this antigen based on the ontogenetic patterns of this antigen expression. In this study, we have performed a detailed immunohistochemical analysis of the developmental expression of this antigen in different stages of the murine embryo. The present study demonstrated initial characterization of the R4-A9 antigen in murine embryogenesis, and the potential functional role of this antigen in hematopoiesis as well as in embryogenesis is discussed.

MATERIALS AND METHODS

Mice

Staged embryos were obtained by mating ICR male and female mice. ICR mice were purchased from the Shizuoka Laboratory Animal Center (Shizuoka, Japan). Mice were maintained in Micro-Isolator cages on hardwood-chip contact bedding and were provided with commercial rodent chow and acidified water (pH2.5). Noon on the day of vaginal plug was considered 1/2 day p.c.[10]

Embryos and tissues

Mice were killed by cervical dislocation and embryos or adult tissues were transferred immediately to ice-cold 4% periodate-lysine-paraformaldehyde (PLP).[11] Early embryos (8 days p.c.) were sectioned within the decidua. Embryos nine days p.c. and older were dissected from the embryonic membranes. Samples were fixed for 8 h at 4°C and incubated in 0.5 mol/L sucrose in phosphate-buffered saline (PBS) at 4°C overnight before embedding in Tissue Tek II (Miles, Naperville, USA). Longitudinal sections (8 μm) of whole embryos were cut and mounted on poly-L-lysine (Sigma Chemical Co., St Louis, MO, USA) coated glass slides. Staging of embryos for descriptive purposes was done according to Kaufman, using plate numbers taken from his *Atlas of Mouse Development.*[12]

Immunohistochemistry

Immunohistochemical studies of tissue sections of staged mouse embryos (N=30, 8, 9, 10, 13½, 16½ and 18 days p.c.) and neonatal mice (N=5, 5 days p.p.) were performed using a previously characterized monoclonal antibody R4-A9.[9] Staining was performed according to an avidin-biotin immunoperoxidase method (Vectastain kit; Vector Laboratories, Burlingame, CA, USA) as follows. Briefly, sections from each gestational day were subjected to immunohistochemistry with the R4-A9 monoclonal antibody or with purified rat IgG (Sigma), all at an equivalent IgG concentration of 5 μg/mL. The primary antibody:antigen complexes were detected using the Vectastain ABC kit (Vector Laboratories). After blocking endogenous peroxidase with 0.3% hydrogen peroxide in methanol, non-specific antibody binding was blocked with normal goat serum (5%) in PBS. The R4-A9 antibody was applied and left overnight at 4°C. The secondary antibody was biotinylated goat anti-rat IgG, and the ABC system protocol was followed using 3, 3'-diaminobenzidine (Wako Pure Chemical Co., Tokyo, Japan) as the chromogen. Sections were counterstained with methyl green. No immunoreactivity was observed in tissues exposed to the secondary antibody alone. Sections stained only with diaminobenzidine tetrahydrochloride showed little or no endogenous peroxidase activity. Results were analyzed by light microscopy for patterns of R4-A9 staining and their correlation with previous studies of this antigen expression in the normal adult mouse.

RESULTS

Immunohistochemical localization of R4-A9 antigen during early embryonic development (8, 9 and 10 days p.c.)

To investigate the distribution of R4-A9 antigen at various stages of development in the mouse, tissues were dissected from 8 days p.c. to 5 days p.p. In our study, R4-A9 antigen was first detected in the embryo at around 8 days p.c. Analysis of transverse sections of 8 days p.c. embryos revealed that a low level of R4-A9 staining could be detected in the yolk sac at this stage (Fig. 1). Furthermore, at this stage, the reaction products were also present in the embryo itself. In this study, weak reaction products could be detected in the myocardial tissues forming the primitive heart tube (Fig. 1).

To further investigate the expression pattern of the R4-A9 antigen in early embryogenesis, transverse sections were prepared at 9 days p.c. The expression of this antigen was

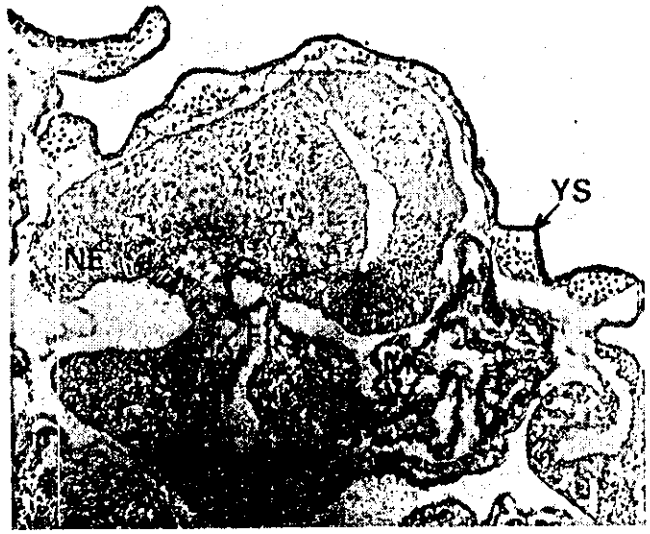

Figure 1 Expression of R4-A9 antigen in a section from an 8 days p.c. mouse embryo stained with R4-A9 antibody. High-power view of the transverse section shows expression of R4-A9 antigen in the myocardial tissue of primitive heart. At this stage, a low level of R4-A9 staining could be detected in the yolk sac. YS, visceral yolk sac; F, pharyngeal region of foregut; MC, myocardial tissue of primitive heart; NE, neuroepithelium in prospective hindbrain region.

clearly detected in mesenchymal cells around the fourth ventricle, the telencephalic vesicle, the otic vesicle and the neural tube. In particular, the distribution of this antigen was restricted to specific areas in the myelencephalon, where the mesoderm under the surface ectoderm accumulated reaction products. At 9 days p.c., R4-A9 antigen could be detected in the developing heart. Immunostaining revealed that antibody staining was seen in the myocardial wall of the atrioventricular region (Fig. 2a,b). In the 10 days p.c. embryo, antibody staining was also found in the embryonic liver (Fig. 3a). Frozen sections of the embryonic liver revealed that high levels of antibody staining were observed in the liver parenchyma (elements of hepatic/biliary primordia).[12] High-power views showed a fine network spreading throughout

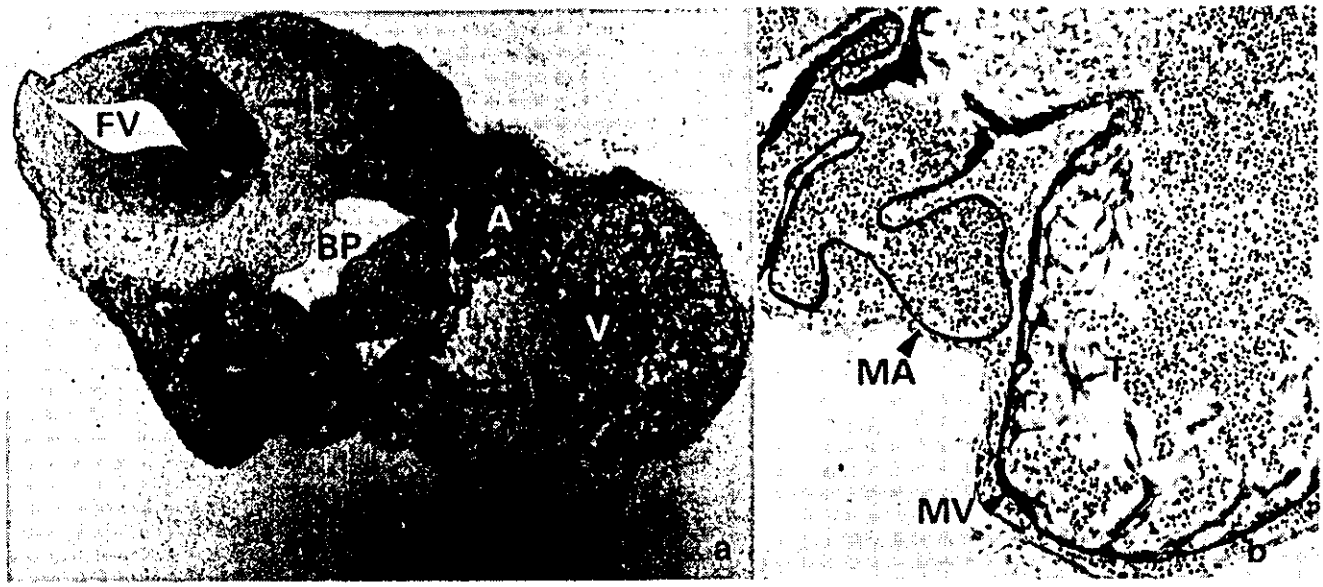

Figure 2 Expression of R4-A9 antigen in sections from a 9 days p.c. mouse embryo stained with R4-A9 antibody. (**a**) Transverse section of the heart and myotome regions of a similar embryo shows expression of R4-A9 antigen in the myocardial wall of the atrioventricular region. (**b**) High-power view of the transverse section in (A) shows morphology of the atrium and ventricle. Erythrocytes are peroxidase-positive. FV, fourth ventricle; BP, second branchial pouch; A, common atrial chamber of heart; V, common ventricular chamber of heart; T, trabeculae; MV, myocardial wall of common ventricular chamber of heart; MA, myocardial wall of common atrial chamber of heart.

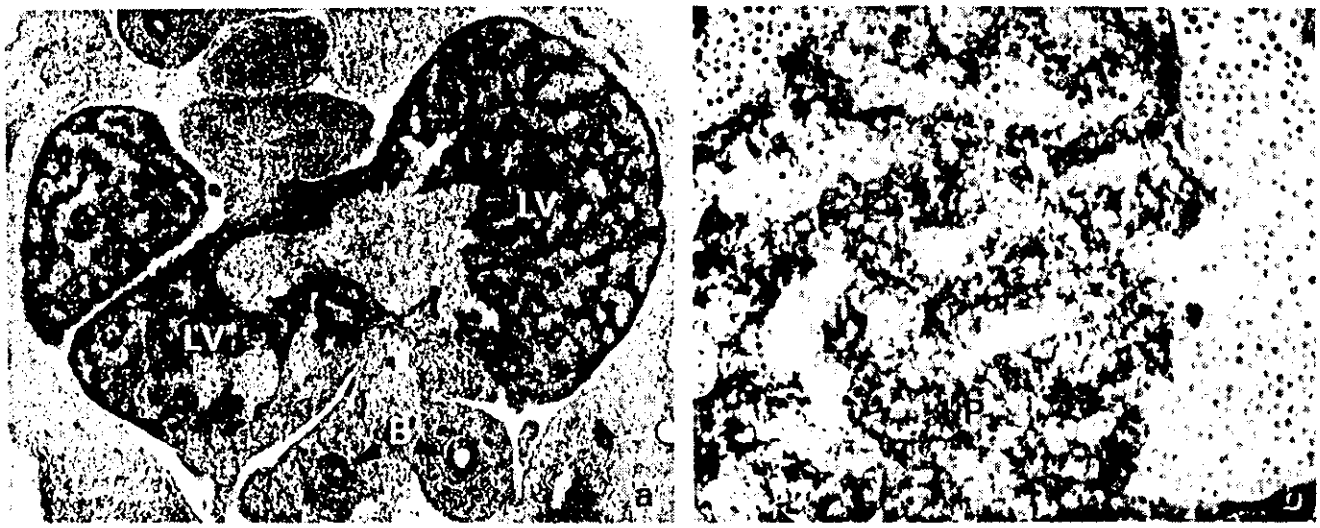

Figure 3 Expression of R4-A9 antigen in sections from a 10 days p.c. mouse embryo stained with R4-A9 antibody. (**a**) Transverse section of a similar embryo at the level of the forelimb buds shows expression of R4-A9 antigen in the embryonic liver. (**b**) High-power view of the transverse section in (A) shows expression of R4-A9 antigen in the liver parenchyma (elements of hepatic/biliary primordia). The R4-A9 positive cells in the liver parenchyma possessed thin processes by which they connected with those of adjacent cells. LV, embryonic liver; B, main bronchus; LP, liver parenchyma.

the liver parenchyma. This network consisted of fibroblastic mesenchymal cells, possessing thin processes by which they connect with those of adjacent cells. No reaction products could be detected in blood cells (Fig. 3b). Additionally, no expression of this antigen could be detected in the neural tube, otic vesicle, brain (telencephalon, metencephalon and myelencephalon) or trigeminal neural crest tissue.

Immunohistochemical localization of the R4-A9 antigen in organogenesis (13½ days p.c.)

This stage is characterized by rapid growth and differentiation of the organ systems. At 13½ days p.c., the mouse embryo is at the peak of organ development. Sagittal and parasagittal sections of the embryo from 13½ days p.c. were immunohistochemically stained with R4-A9 antibody. After 10 days p.c., the fetal liver rapidly becomes the major site of fetal hematopoiesis.[13,14] In our study, high levels of antibody staining could be detected in the embryonic liver at 13½ days p.c. High-power microscopy revealed that the expression of this antigen was found in the mesenchymal cells supporting the liver parenchyma (Fig. 4a). Between blood vessels, the positive cells possessed slender cytoplasmic processes that extended between neighboring developing cells. These processes were thought to be connected with each other to form a cellular reticulum. No reaction products could be detected in blood cells in the blood vessels (Fig. 4c). R4-A9 also reacted with the vascular walls of central veins. The positive cells were connected with each other to form a

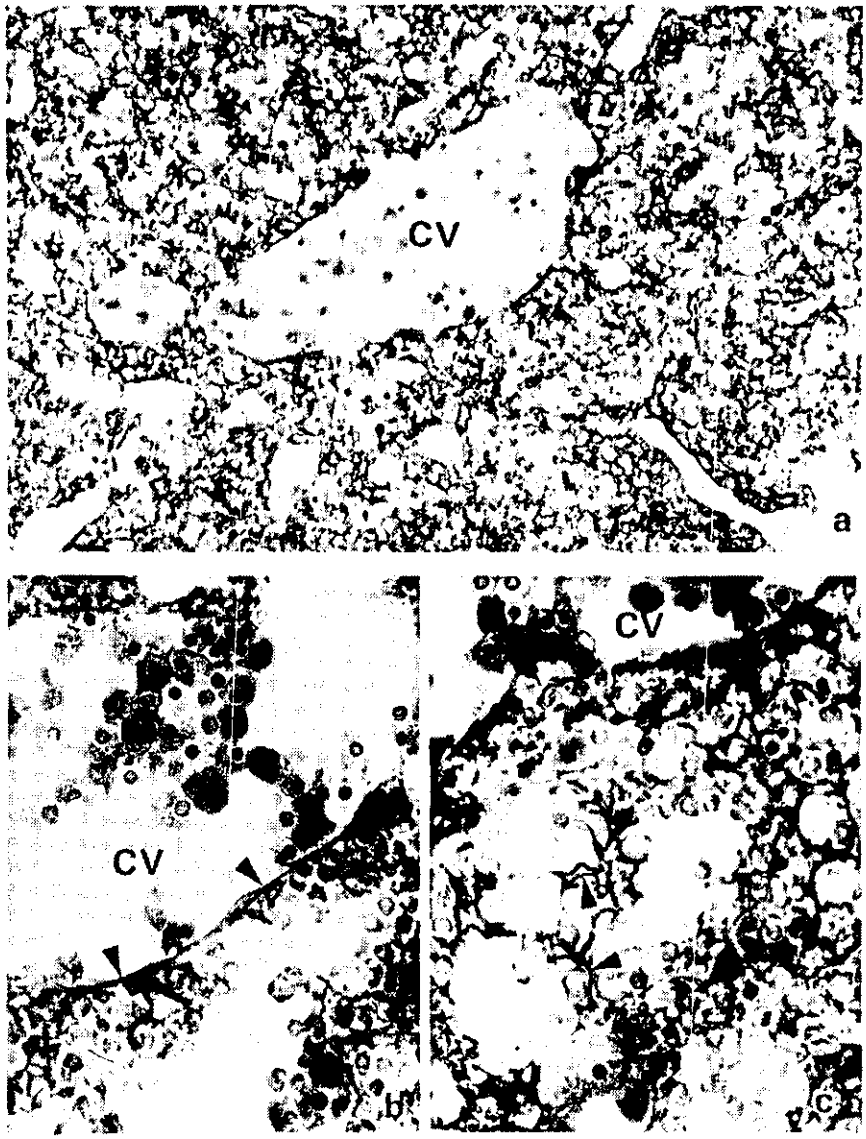

Figure 4 Expression of R4-A9 antigen in sections from a 13½ days p.c. mouse embryo stained with R4-A9 antibody. Parasagittal section of a 13½ days p.c. embryo. (**a**) High-power view of the liver shows the expression in the mesenchymal cells supporting liver parenchyma. (**b**) The positive cells (arrowheads) in the vascular walls of central veins are connected with each other to form a single layer. (**c**) Between blood vessels, the positive cells (arrowheads) possess slender cytoplasmic processes that extend between neighboring developing cells. Note the absence of expression in blood cells in the blood vessels. Erythrocytes are peroxidase-positive. CV, central vein.

single layer on the vascular walls of central veins. Although difficult to discern clearly in frozen sections, R4-A9-positive cells in the vascular walls seemed to correspond to the endothelium from their immunohistochemical distribution pattern (Fig. 4b). This staining pattern in the liver was seen as early as 10 days p.c. and remained consistently high in the mesenchymal cells until late in gestation at 18 days p.c. At around 13½ days p. c., antibody staining was also present on a class of medullary (probably stromal) cells in the thymus (Fig. 5a).

No staining was seen in the developing central nervous system of the mouse, including the spinal cord and brain (cerebellum, hippocampus and telencephalon). Exceptionally, moderate staining for this antigen could be detected in the choroid plexus. Analysis of the choroid plexus by high power microscopy revealed that this immunoreactivity was seen mainly in the netlike structure of the capillary-rich mesenchyme, but not in the epithelium of the choroid plexus. Light staining for this antigen was also observed in a thin layer of meninges surrounding the brain, whereas by 18 days p.c., this antigen staining was lost, concomitant with differentiation of the meninges.

An additional but major feature of our results from 12 to 15 days p.c. was the expression of this antigen in the mesenchyme *per se* or in tissues derived from the mesenchyme in some organs. In these instances, particularly intense staining of the mesenchyme without staining of the epithelium was seen. Further examples were found in the developing intestine, where staining was seen only in the submucosa, but not in mucosal epithelial cells, and in the embryonic skin, where high levels of staining were seen only in the dermis bounded by an adjacent epidermis, but not in the epidermis. High power views of this section showed that high levels of antibody staining were observed in a single layer of dermal fibroblasts (Fig. 5b).

Immunohistochemical localization of the R4-A9 antigen in late organogenesis (16½ days p.c.)

From 15 to 17 days p.c., the liver remains the major site of hematopoiesis. Sagittal sections of 16½ day old embryos showed that the largest mass expressing this antigen was the embryonic liver. Although the positive regions for the R4-A9 antigen were diffusely distributed throughout the liver, antibody staining was noted in mesenchymal cells both in the parenchyma and sinusoids. In this section, no staining of this antigen could be seen in blood cells. At 16½ days p.c., antibody staining remained positive in a restricted pattern in the medulla of the thymus.

From 13 to 17 days p.c., the heart becomes well differentiated, and the ventricles and atrium remained positive for the antibody (Figs 6a,7a). At 16½ days p.c., we observed a higher level of expression in the subepicardial layer of the ventricular myocardium compared with the trabecular layer and epicardium (Fig. 6a).

Figure 5 Expression of R4-A9 antigen in sections from a 13½ days p.c. mouse embryo stained with R4-A9 antibody. (**a**) Section of a similar embryo showing expression in a class of medullary cells in the thymus. (**b**) High-power view of the skin in a similar embryo showing expression in a thin layer of dermal fibroblasts (arrowheads), but not in the epidermis. D, dermis; ED, epidermis.

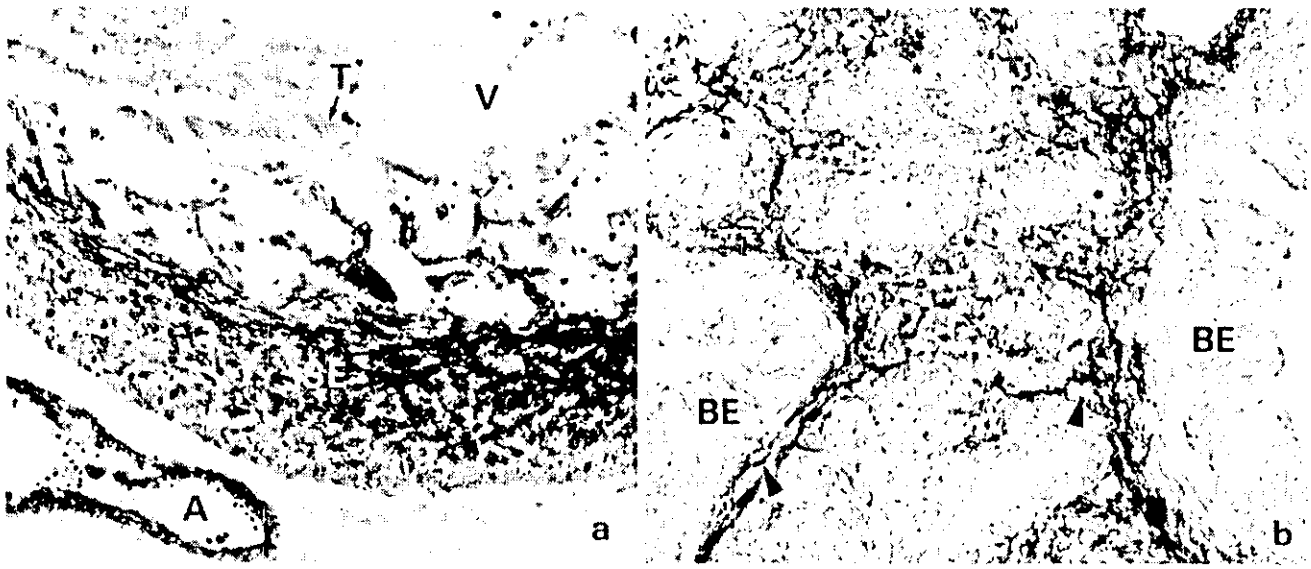

Figure 6 Expression of R4-A9 antigen in sections from a 16½ days p.c. mouse embryo stained with R4-A9 antibody. (**a**) High power micrograph of the heart in a similar embryo. Low levels of staining were localized in the trabecular layer and epicardium of the ventricle, but higher levels were seen in the subepicardial layer of ventricular myocardium. Erythrocytes were peroxidase-positive. (**b**) High power micrograph of the lung in a similar embryo. Staining was detected in the fibroblasts (arrowheads) surrounding the epithelium of the bronchiole as well as in the subepithelial region of the lung parenchyma. A, atrium; V, ventricle; T, trabeculae; SE, subepicardial layer of the ventricular myocardium; BE, bronchiolar epithelium.

Analysis of sagittal sections from embryos aged 16½ days p.c. revealed that the mesenchyme itself, or tissues derived from the mesenchyme, continued to express the R4-A9 antigen. As for the lung, high levels of staining for this antigen could be detected in the fibroblasts surrounding the cuboidal epithelium, but not in the cuboidal epithelium (Fig. 6b). Expression of this antigen was also found in the embryonic kidney. At 16½ days p.c., this antigen staining was present in a very restricted pattern in the subepithelial region of the tubule epithelium, but not in the tubule epithelium itself. However, this positivity became visible shortly before birth and was no longer present after birth.

Interestingly, particularly intense staining was detected when remodeling of the mesenchyme or mesoderm occurred, as during formation of the digits from limb buds and the tail (Fig. 7a,b,c). High power microscopy revealed that antibody staining was preferentially localized in the dermal fibroblasts bounded by an adjacent epidermis. In contrast, no staining could be detected in the developing bone and cartilage. Overall, it appears that the expression of the R4-A9 antigen in the mesenchyme, where R4-A9 staining was greatest between days 13 and 15, decreased in intensity at late organogenesis.

Immunohistochemical localization of the R4-A9 antigen from 18 days p.c. to 5 days p.p.

At 18 days p.c., R4-A9 antigen was still present in the liver and thymus, but was increasingly apparent in the bone marrow and spleen, which are the predominant sites of hematopoiesis at birth and during postnatal development. In the bone marrow, at this stage, R4-A9 positive fibroblastoid (probably stromal) cells were the first to invade the marrow, and then these positive cells delineated lumina loaded with scanty hematopoietic cells. High power views of this section showed that high levels of antibody staining were observed in the walls of the vascular sinus (Fig. 8a). In the spleen, at 5 days p.p., R4-A9 staining could be seen in the mesenchymal cells supporting the splenic parenchyma (Fig. 8b). Likewise, positive staining was found in the mesenchymal cells supporting parenchyma of the Peyer's patch at 18 days p.c. to 5 days p.p. (Fig. 9a), whereas this immunoreactivity was no longer present from 10 days after birth (Fig. 9b). Surprisingly, after birth, R4-A9 staining was increasingly apparent both in bone marrow and spleen, with a concomitant decrease in staining of the liver.

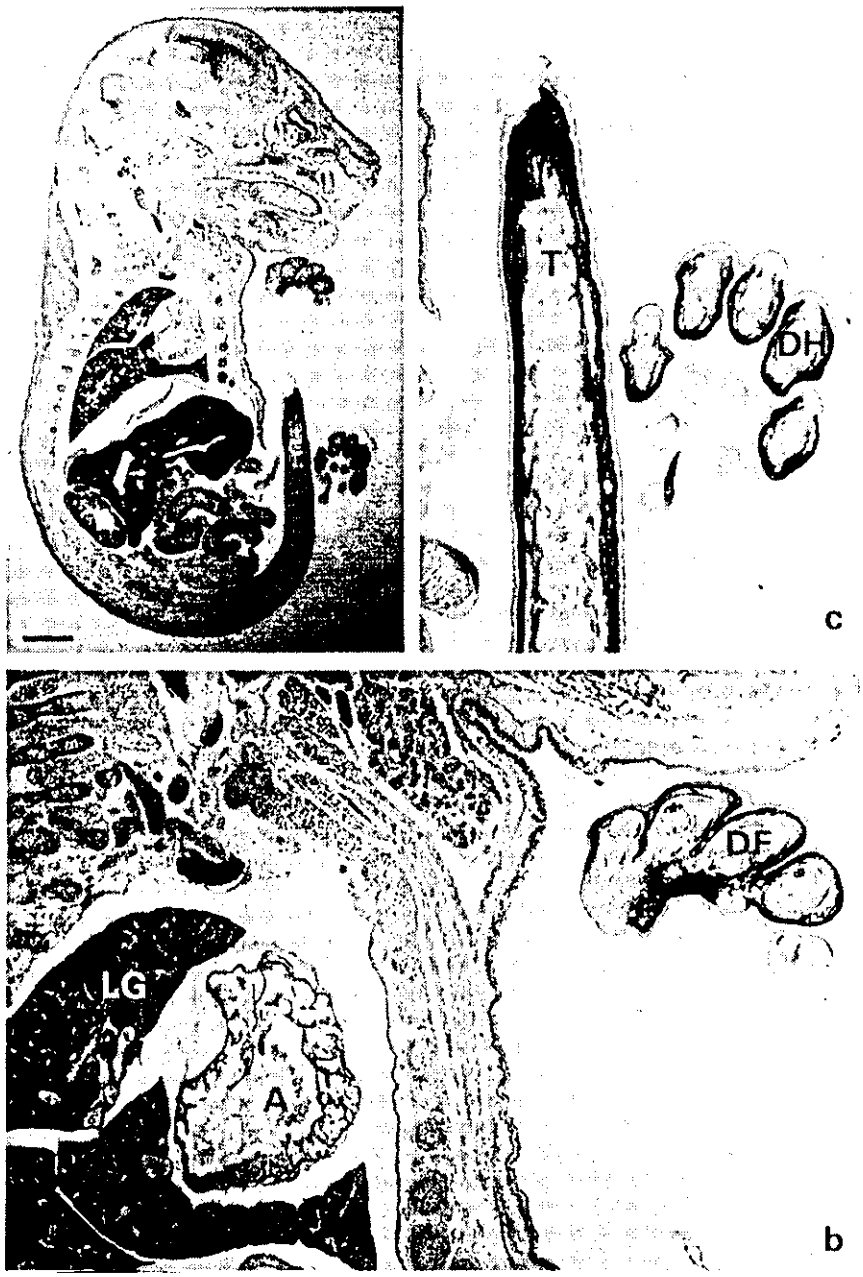

Figure 7 Expression of R4-A9 antigen in sections from a 16½ days p.c. mouse embryo stained with R4-A9 antibody. (**a**) Sagittal section from a 16½ days p.c. embryo stained with R4-A9. Bar=2 mm. (**b**) Parasagittal section of a similar embryo to show expression in digits. Staining was also seen in the lung and atrium. (**c**) Parasagittal section of a similar embryo to show expression in the digits as well as in the tail. DF, digits of forelimb; DH, digits of hindlimb; T, distal part of tail; A, right atrium; LG, right lung.

At 18 days p.c., liver tissues show mature sinusoid/parenchymal organization, the hepatocytes become more cohesive and liver cords develop. At this stage, positive staining in the fetal liver was further reduced from that seen at 16½ days p.c. Analysis of the liver by high power microscopy revealed that antibody staining could be detected in the sinusoidal walls. R4-A9-positive cells in the walls were thought to be connected with each other to form a thin layer surrounding the hepatocytes. Although difficult to discern clearly in frozen sections, the positive cells in the sinusoidal walls seemed to correspond to the endothelium from their immunohistochemical distribution pattern (Fig. 10a). In contrast, no staining could be seen in either blood cells or hepatocytes. At 18 days p.c., small amounts of R4-A9 antigen were

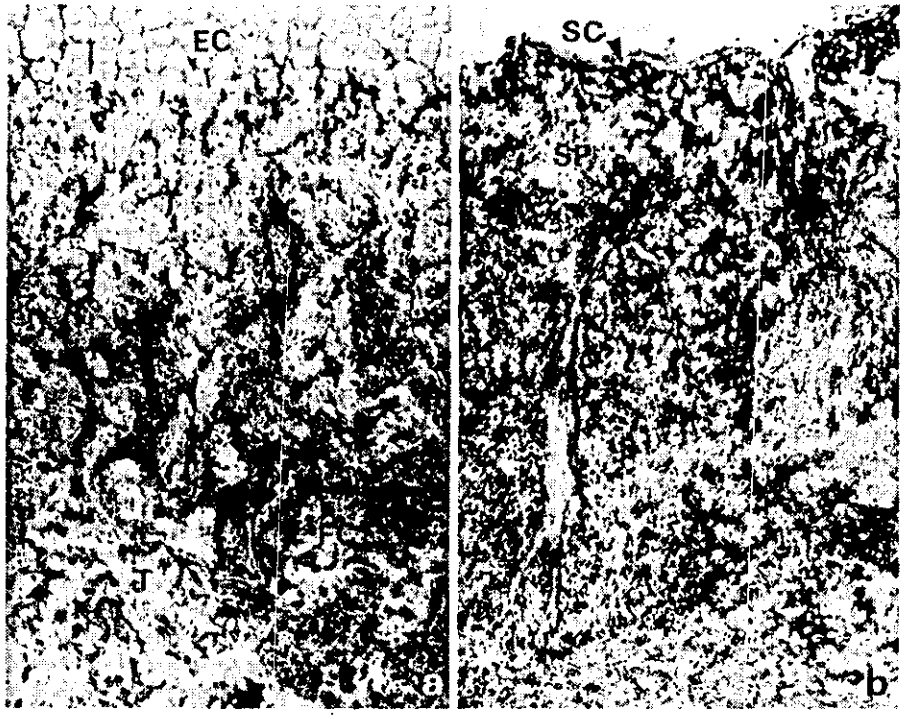

Figure 8 Expression of R4-A9 antigen in the mouse at 18 days p.c. and 5 days p.p. (**a**) Cross section through the ribs of an 18 days p.c. embryo. Staining is seen primarily in a few fibroblastoid cells in the bone marrow. High-power views of this section showed high levels of antibody staining in the walls of the vascular sinus. (**b**) Section of a spleen from a 5 days p.p. mouse. Staining was seen in the mesenchymal cells supporting the parenchyma of the splenic red pulp. T, trabeculae; FC, fibroblastoid cell; EC, epiphyseal cartilage; SP, splenic parenchyma; SC, splenic capsule.

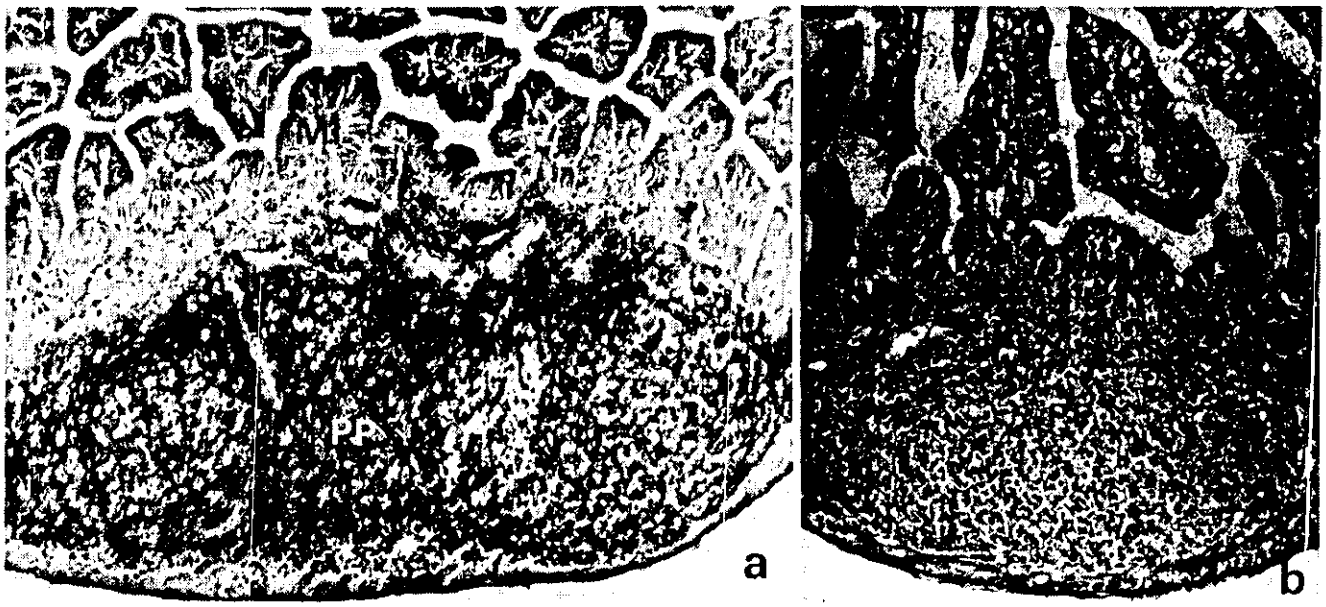

Figure 9 Expression of R4-A9 antigen in the mouse at 18 days p.c. and 5 days p.p. (**a**) Section of the Peyer's patch in the large intestine of an 18 days p.c. embryo. Staining was seen in the mesenchymal cells supporting the parenchyma of the Peyer's patch. (**b**) Section of the Peyer's patch in large intestine 5 days after birth. Note the absence of expression in the Peyer's patch. MI, mucosa of large intestine; PP, Peyer's patch.

observed in the medullary area of the thymus as regional clusters of positivity (Fig. 10b). This antibody staining in the liver and the thymus remained consistent until 5 days after birth and was no longer present in adult mouse tissues. In the testis, R4-A9 staining of the Leydig cells could be detected from 5 days after birth.

At 18 days p.c., low levels of antigen expression could be seen where there was remodeling of the mesenchyme, as during formation of digits from limb buds, observed already at 16½ days p.c. By late gestation at 18 days p.c., other mesodermic elements, like mesenchymal connective tissues, retained positivity. However, this positivity became visible shortly before birth and was no longer present from 10 days after birth.

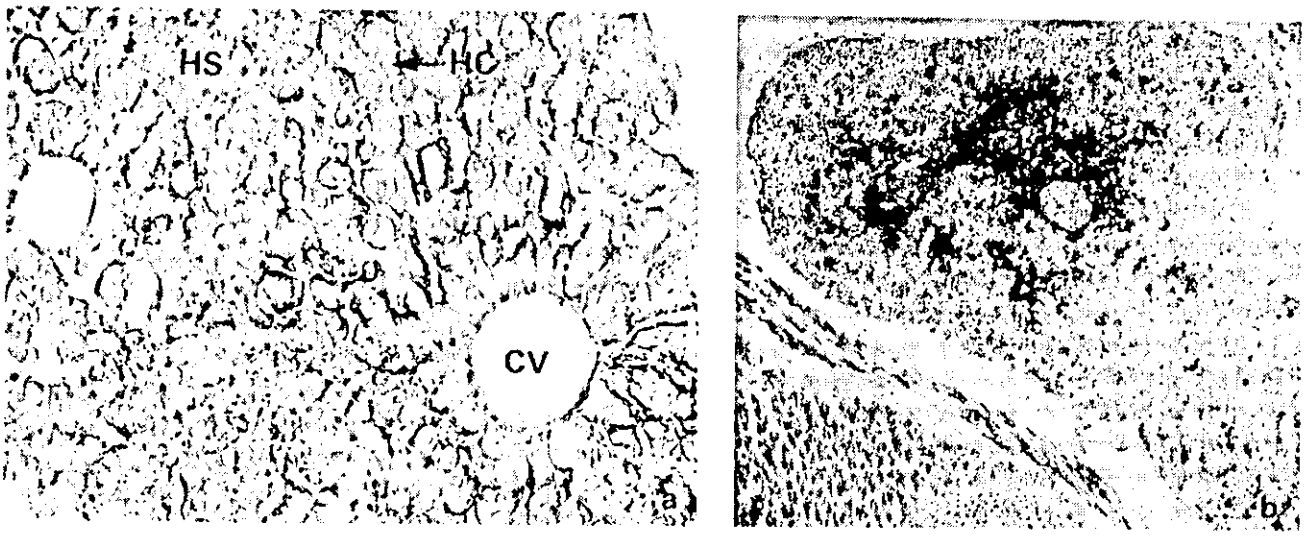

Figure 10 Expression of R4-A9 antigen in sections from an 18 days p.c. mouse embryo stained with R4-A9 antibody. (**a**) Section of a liver showing expression in the sinusoidal walls. R4-A9-positive cells are apparently connected with each other to form a thin layer surrounding the hepatocytes. Note the absence of expression in both blood cells and hepatocytes. (**b**) Section of a thymus showing expression in the medullary area of the thymus as regional clusters. HC, hepatocyte; CV, central vein; HS, hepatic sinusoid.

Table 1 Expression of the R4-A9 antigen in murine tissues during embryogenesis and the neonatal period

	Developmental stage (days)								
	Post-coitum						Post-partum		
Tissue	8	9	10	13½	16½	18	1	5	10
Yolk sac	+								
Liver		+	++	+++	+++	++	+	+	–
Thymus			+	++	++	+	+	+	–
Lymph node					+	++	+	+	–
Spleen						+	++	++	++
Bone marrow						+	++	++	++
Testis								+	+
Heart		+	++	+++	++	+	–	–	–
Skin				++	++	+	+	+	–
Lung				++	++	+	–	–	–
Kidney				+	++	+	–	–	–

–, no reactivity; +, low; ++, moderate; +++, high.

DISCUSSION

We hypothesized that the R4-A9 antigen, a specific marker of bone marrow stroma in adult mice, would also be expressed in hematopoietically active organs in embryonic mice. As would be expected, we observed that the expression of this antigen was clearly present in the mesenchymal cells that support hematopoiesis, such as the embryonic liver and the thymus. Coupled with our previous data, our present study in a manner indicates that R4-A9 antigen is a specific marker of hematopoietic stroma both in the fetus and the adult. Furthermore, this result is consistent with the suggestion by Friedenstein *et al.* that hematopoietic stromal cells may carry determinants that are specifically related to the presence of hematopoiesis.[15,16]

From 12 to 15 days p.c., R4-A9 staining was increasingly apparent in the embryonic liver. At this time, hematopoietic development shifts from its extra-embryonic hematopoietic locus to the liver, and then hematopoiesis begins in the intra-embryonic site.[13,14] However, a surprising but major finding was that, concomitant with the decreasing expression of R4-A9 antigen in the liver, increasing expression of this antigen was observed in bone marrow and spleen. Therefore, the apparent association of this antigen's expression with embryonic hematopoiesis suggests that its expression is coordinately regulated at the developmental stages of the sites of embryonic hematopoiesis.

Unexpectedly, detailed analysis of the localization of the R4-A9 antigen at 13½ days p.c. revealed that this antigen was not only expressed in hematopoietic tissues but also in